UNIVERSIDADE D
COIMBRA

Ana Sofia Alberto e Silva

ELECTROPHYSIOLOGICAL VALIDATION AND CHARACTERIZATION OF PHARMACOLOGICAL COMPOUNDS TARGETING GLUK2/GLUK5 KAINATE RECEPTORS

Dissertação no âmbito do Mestrado em Biologia Celular e Molecular, com especialização em Neurobiologia, orientada pelo Professor Doutor Christophe Mulle e pelo Professor Doutor Carlos Duarte, apresentada ao Departamento de Ciências da Vida da Faculdade de Ciências e Tecnologia da Universidade de Coimbra.

Outubro de 2020

UNIVERSIDADE D
COIMBRA

Faculty of Sciences and Technology of the University of Coimbra

Department of Life Sciences

Master of Science in Cellular and Molecular Biology

Ana Sofia Alberto e Silva

Electrophysiological validation and characterization of pharmacological compounds targeting GluK2/GluK5 kainate receptors

Supervisors:
Christophe Mulle (at Institute for Interdisciplinary Neuroscience)
Carlos Duarte (at Department of Life Sciences)

October of 2020

The following work occurred in "Synaptic Circuits of Memory" Lab, headed by Dr. Christophe Mulle, and located at the Institute for Interdisciplinary Neuroscience, being part of the Bordeaux Neurocampus Department of the University of Bordeaux (Bordeaux, France). The work was conducted under the co-supervision of Dr. Christophe Mulle and Dr. Gaël Barthet. Previous agreement for Erasmus+ Mobility Program was established between the University of Coimbra and the University of Bordeaux. This work was financially supported by the University of Bordeaux, the French National Centre for the Scientific Research and the Network of European Funding for Neuroscience Research (KARTLE Project). Additionally, it relied on a collaboration with Dr. Bernard Pirotte's Lab at the University of Liège (in the scope of KARTLE Project).

ACKNOWLEDGMENTS

It comes the time to think about this journey since the beginning, this is, September of 2019, around one year ago. It is challenging to put into words all my gratitude towards my host laboratory at the Institute for Interdisciplinary Neuroscience (IINS), the friends I made along the way and all the family and friends living in Portugal (and in other countries!), who supported me every single day since I arrived Bordeaux.

Now, back in Portugal, not so long ago, I can say I went to Bordeaux without any kind of expectations. We all know how it works, don't we? And… What an incredible surprise I had! Despite knowing I was going to work in a research field I truly liked, in a research team I admired and with many different research topics which interested me, I also found a very welcoming working environment, which transformed this experience of being abroad (for a long period) a very enjoyable experience.

You, people in Mulle team, are the first people I would like to say thank you. Starting of course with the head of the team, Christophe Mulle, for accepting me in your group to develop this Master thesis and for the trust having me working in the laboratory for some extra months after the first wave of the SARS-CoV-2 pandemic. Also, thanks for valuing so much my work in your team, it has meant a lot to me. All this experience I gained in your lab will be something I will always keep with me and value in my scientific career. *Merci beaucoup!*

From the people sit right next to me in "my" office to the people in the neighbour offices, I'd like to thank Gaël Barthet, my daily co-supervisor at IINS, for all the patience explaining me every procedure before, during and after patch-clamp in *ex-vivo* slices, and for helping me at any time, even when you were very busy with other tasks; Thank you very much Júlio Viotti for all the availability, kindness and calmness explaining me many concepts in electrophysiology too, helping me when I was in troubles, and for always finding me a solution! With you, I learnt that there is a solution for every problem, literally; To Tomàs Jordà-Siquier (aka Jordsi), thank you a lot for making me laugh after I came from the electrophysiology setup without any good cell to analyse. Your optimism is contagious and indeed you made some of my days much easier; To Ânia Gonçalves, thanks for the support, for all the advice regarding future perspectives, and for updating me in comedians all around the world; Dario Cupolillo, Catherine Marneffe, Ashley Kees, Séverine Deforges, Noëlle Grosjean, Thierry Amédée, Justine Gautron, Ruth Betterton, Amandine Papin, Jay Panji and Emeline Muller, thank you very much to each one of you for all the moments shared, lessons learnt and experiences together. Each one of you somehow impacted and importantly shaped my journey in Bordeaux. I will be forever grateful also to you. Still, thanks to all the research technicians, PhD students and postdocs I met at IINS who

promptly helped me at any time. Special thanks to Rémi Sterling for teaching me important procedures in cell culture.

To my dear colleague and friend Ana Marta Capaz, thank you so much for listening to me at the end of each day after work. The confinement somehow broke our common living in the same flat, but I am happy we shared it for some months! *Muito obrigada, amiga!*

A big thank you to all the Portuguese community set in Bordeaux and not mentioned yet in this text, with a special thanks to Alexandra Fernandes for welcoming me in the first days so well, offering her place for so many cool parties, and for exploring with me some artistic events around Bordeaux; to Filipe Nunes Vicente for showing me the most random contents (but always very good!); and also to Inês Delgado who helped me a lot in health-related issues in France. *Obrigada a todos!*

Last but not the least, I would like to thank Prof. Ana Luísa Carvalho and Prof. Carlos Duarte for their work as teachers in the Master in Cellular and Molecular Biology. You have inspired me to work every single day, even harder, to reach my goals in science. Also, thanks for all the support given during my stay abroad and for the constant availability to help in any issue.

Finally, but now in Portuguese…

Para todos os que sabem o meu percurso até aqui: parar a minha vida profissional para voltar a estudar aos 25 anos não foi uma decisão fácil de ser tomada, mas tenho a certeza que valeu a pena por tudo aquilo que aprendi, continuo a aprender, e pelas pessoas que conheci e continuo a conhecer. Estamos sempre a tempo de lutar por aquilo que nos faz felizes. Por isso, tentem, e, talvez, sejam mesmo muito felizes. Seja em que área for. Pessoal ou profissionalmente. Nunca é tarde de mais. Um bem-haja a todos!

Ana Sofia Silva

TABLE OF CONTENTS

LIST OF ABBREVIATIONS

A/C fibers – Associational/ commissural fibers
ACSF – Artificial cerebrospinal fluid
AED – Anti-epileptic drug
AMPA – A-amino-3-hydroxy-S-methylisoxazole-4-propionic acid
AMPAR – A-amino-3-hydroxy-S-methylisoxazole-4-propionic acid receptor
BBB – Blood brain barrier
CA1/3 – Cornu ammonis 1/3
CaMKII – Calcium/ calmodulin-dependent protein kinase II
cDNA – Complementary deoxyribonucleic acid
CNS – Central nervous system
CTD – C-terminal domain
DG – Dentate gyrus
DGC – Dentate granule cell
DKO – Double knockout
DMSO – Dimethyl sulfoxide
DRG – Dorsal root ganglion
EC – Entorhinal cortex
EC_{50} - Half maximal effective concentration
EPSCs – Excitatory postsynaptic currents
FF – Frequency facilitation
GCD – Granule cell dispersion
GWAS – Genome-wide association studies
IC_{50} – Half maximal inhibitory concentration
iGluRs – Ionotropic glutamate receptors
ILAE – International League Against Epilepsy
I_{NaP} – Persistent sodium current
KA – Kainate
KAR – Kainate receptor
KO – Knockout
LBD – Ligand binding domain
LTD – Long-term depression
LTP – Long-term potentiation
MF – Mossy fiber
mGluRs – Metabotropic glutamate receptors
MRI – Magnetic resonance imaging
mTLE – Mesial temporal lobe epilepsy
NETO1 – Neuropilin Tolloid-like 1
NETO2 – Neuropilin Tolloid-like 2
NMDA – N-methyl-D-aspartate
NMDAR – N-methyl-D-aspartate receptor
NTD – N-terminal domain
nTLE – Neocortical temporal lobe epilepsy
PAM – Positive allosteric modulator
PC – Pyramidal cell
PKC – Protein kinase C
PP – Paired-pulse
PSD – Postsynaptic density
PTX – Pertussis toxin
rMF – Recurrent mossy fiber
RT – Room temperature
sAHP – Slow after-hyperpolarizing potential
SAR – Structure-activity relationship
SE – Status epilepticus
TE – Thorny excrescence
TLE – Temporal lobe epilepsy
TMD – Transmembrane domain
UBP – University of Bristol Pharmaceuticals
WES – Whole exome sequencing
WGS – Whole genome sequencing
WT – Wild type

RESUMO

Os recetores de cainato (KARs) são recetores de glutamato ionotrópicos tetraméricos, com caraterísticas biofísicas distintas, que regulam a atividade dos circuitos sinápticos a nível pré-sináptico e pós-sináptico através de ações ionotrópicas e/ou metabotrópicas. Estes recetores podem formar combinações homoméricas ou heteroméricas constituídas por diferentes subunidades do tipo GluK1–GluK5. Em mamíferos, o KAR heteromérico GluK2/GluK5 é o subtipo de KAR mais abundante no cérebro. Aquando da sua ativação por glutamato libertado endogenamente, os KARs GluK2/GluK5 medeiam correntes pós-sinápticas excitatórias (EPSCs) de cinética lenta e baixa amplitude, tendo um papel importante na transmissão sináptica excitatória e na integração sináptica.

A necessidade atual de validar e caracterizar novos compostos farmacológicos que possam atuar seletivamente nos KARs surgiu naturalmente de forma a melhor entender as funções fisiológicas desta família de recetores de glutamato e também para melhor explorar o seu impacto na patofisiologia de algumas doenças neurológicas, tais como a epilepsia e a dor neuropática. Esta tese de Mestrado tem como objetivo validar e caracterizar novos antagonistas ortostéricos putativos e moduladores alostéricos putativos dos KAR GluK2/GluK5 usando eletrofisiologia em fatias de cérebro e aplicando diferentes protocolos de eletrofisiologia. Estes compostos farmacológicos foram sintetizados e fornecidos por um colaborador do projeto KARTLE (Laboratório do Dr. Bernard Pirotte – Universidade de Liège, Bélgica). Todo o conjunto de experiências foi realizado num contexto sináptico, especificamente nas sinapses das fibras musgosas com os neurónios da região Cornu ammonis 3 (sinapses mf-CA3) no hipocampo. Entre os dois grupos principais de compostos farmacológicos testados, o grupo de antagonistas ortostéricos putativos mostrou ter um impacto maior na redução quer da amplitude máxima quer da carga elétrica sináptica das EPSCs mediadas por KARs (KAR-EPSCs) nas sinapses mf-CA3. Neste grupo, verificou-se que o composto experimental P03, na concentração testada, foi mais potente que o composto de referência UBP310 em reduzir a carga elétrica sináptica mediada por KARs, indicando que este poderá ser um novo composto líder a atuar nos KARs GluK2/GluK5. Antecipamos que este e outros potenciais novos compostos farmacológicos que atuem nos KARs GluK2/GluK5 possam servir como ferramentas para melhor caraterizar as suas funções fisiológicas e representar opções adicionais para novas abordagens terapêuticas.

Palavras-chave: *compostos farmacológicos; eletrofisiologia em fatias de cérebro; KAR-EPSCs; KARs GluK2/GluK5; sinapses mf-CA3.*

ABSTRACT

Kainate receptors (KARs) are tetrameric ionotropic glutamate receptors, with distinct biophysical features, which regulate the activity of synaptic circuits at presynaptic and postsynaptic levels through ionotropic and/or metabotropic actions. They can co-assemble as homomeric or heteromeric combinations of different GluK1–GluK5 subunits. In mammals, heteromeric GluK2/GluK5 KAR is the most abundant KAR subtype in the brain. Upon its activation by endogenously released glutamate, GluK2/GluK5 KARs participate in excitatory postsynaptic currents (EPSCs) with slow kinetics and small amplitude, having an important role in the overall excitatory synaptic transmission and synaptic integration.

The current need of validating and characterizing new pharmacological compounds which can selectively target KARs came naturally in order to better understand the physiological functions of this family of glutamate receptors and also to further explore their impact on the physiopathology of some neurological disorders, such as epilepsy or neuropathic pain. This Master project aims to validate and characterize new putative orthosteric antagonists and allosteric modulators of GluK2/GluK5 KARs using brain slice electrophysiology and applying different electrophysiology protocols. These pharmacological compounds were synthesized and provided by a KARTLE project collaborator (Dr. Bernard Pirotte's Lab – University of Liège, Belgium). The whole set of experiments was performed in a synaptic context, specifically at hippocampal mossy fiber to Cornu ammonis 3 (mf-CA3) synapses. Among the two main groups of pharmacological compounds tested, the group of putative orthosteric antagonists showed a higher impact reducing both peak amplitude and synaptic charge of EPSCs mediated by KARs (KAR-EPSCs) at mf-CA3 synapses. Within this group, we found that the experimental compound P03, in the tested concentration, was more potent in reducing the synaptic charge than the reference compound UBP310, indicating that it may be a new lead compound targeting GluK2/GluK5 KARs. We anticipate that potential new pharmacological compounds targeting GluK2/GluK5 KARs will be able to serve as tools to better characterize these KARs subtype physiologically and may represent additional options for novel therapeutic approaches.

Keywords: brain slice electrophysiology; GluK2/GluK5 KARs; KAR-EPSCs; mf-CA3 synapses; pharmacological compounds.

I. INTRODUCTION

1. KAINATE RECEPTORS (KARs)

1.1. A general overview of excitatory neurotransmission

Glutamate is the main excitatory neurotransmitter in the vertebrate brain, participating in major aspects of normal brain function, including cognition, learning and memory. Glutamate exerts its actions through two distinct class of receptors: the ionotropic glutamate receptors (iGluRs) and the G-protein-coupled metabotropic receptors (mGluRs).

The iGluRs include a-amino-3-hydroxy-S-methylisoxazole-4-propionic acid (AMPA) (GluA1–GluA4), N-methyl-D-aspartate (NMDA) (GluN1–GluN3), kainate (KA) (GluK1–GluK5), and delta (GluD1– GluD2) families of receptors (Carta *et al.,* 2014; Traynelis *et al.*, 2010). While AMPA receptors (AMPARs) mediate fast neurotransmission at the postsynaptic site, NMDA receptors (NMDARs) regulate synaptic transmission and are involved in synaptic plasticity as well as cell survival at extrasynaptic sites. GluD2 is exclusively localized at the postsynaptic site of cerebellar Purkinje cells and gates long-term depression (LTD) of synaptic plasticity (Kohda *et al.*, 2013). Kainate receptors (KARs), despite their structural and functional commonalities with other iGluRs family members, play roles in the brain that are quite distinct from them, having an important role in the regulation and plasticity of neuronal circuits. These functional roles will be further explored in the next sections.

1.2. Genes, nomenclature and structure

KARs are homomeric or heteromeric tetramers assembled from different combinations of five subunits named GluK1-GluK5 (firstly named GluR5–7 and KA1–2). Therefore, current subunit names mirror the corresponding gene names: *GRIK1*, *GRIK2*, *GRIK3*, *GRIK4* and *GRIK5* (Jane *et al*., 2009). Functional KARs comprise four subunits which are assembled from two dimers of two homo- or two heteromeric subunits (Larsen & Bunch, 2011). While GluK1-3 can form homomeric and heteromeric receptors, GluK4-5 require heteromeric assembly with one of the GluK1-3 subunits to form functional channels. GluK1-3 have been termed the low-affinity KARs and GluK4-5 the high affinity KARs (Møllerud *et al.,* 2016). For instance, for kainate, K_D = 5–15 nM for GluK4 and GluK5 and K_D = 70–100 nM for GluK1-3 (Vincent and Mulle, 2009). Overall, this results in receptors with distinct pharmacological and kinetic properties (Ruiz *et al.,* 2005).

The structural diversity of KARs is enhanced by the presence of splice variants for GluK1-3 with variable cytoplasmatic domains. In addition, the GluK1 and GluK2 subunits are subject to

mRNA enzymatic editing, leading to an alternate incorporation of an important amino acid in the channel pore-forming P-loop (the glutamine/arginine (Q/R) site), resulting in reduced divalent cation permeabilities and very low single-channel conductances in the edited version (arginine) (Fig. 1, top image) (Carta *et al.*, 2014). Interestingly, it has been reported an upregulation of GluK2 editing in human seizures, which might be a possible mechanism to reduce seizure vulnerability in an epilepsy context (Vincent and Mulle, 2009).

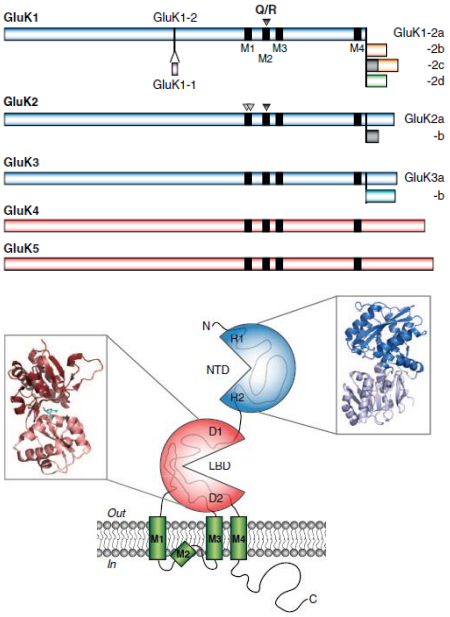

Figure 1 | KAR subunit diversity and structure. Top image: KAR subunits (GluK1–5) and splice variants. Black boxes represent membrane domains (M1–M4). Triangles depict sites of RNA editing, including the Q/R site within both GluK1 and GluK2. **Bottom image:** KAR subunit topology. Crystal structures of the NTD and the LBD are shown (Adapted from Contractor *et al.,* 2011).

KAR subunits were first cloned in the early 1990s and each one displays a similar structure: an extracellular N-terminal domain (NTD), involved in subunit recognition and crucial for the oligomerization of tetrameric receptors, a ligand binding domain (LBD), a helical transmembrane domain (TMD), with three transmembrane α-helices and a re-entrant loop, and an intracellular highly flexible C-terminal domain (CTD), interacting with a number of proteins involved in receptor trafficking and kinetic properties (Carta *et al.,* 2014; Contractor *et al.,* 2011). Each LBD contains two subdomains, D1 and D2, forming a clamshell-like structure with the agonist-binding site located between D1 and D2, and two adjacent D1 domains forming the LBD dimer interface. Upon agonist binding, D2 moves toward D1, transferring a conformational strain to the TMD, which promotes channel opening (Fig. 1, bottom image) (Larsen *et al.,* 2017).

Moreover, post-translational modification of KAR subunits by phosphorylation, palmitoylation and, most recently described, SUMOylation, further increases structural diversity and have an impact on receptor trafficking and function in diverse fashions. Finally, the transmembrane proteins Neuropilin Tolloid-like 1 and Neuropilin Tolloid-like 2 (NETO1 and NETO2) have been identified as KAR auxiliary subunits (Contractor *et al.,* 2011). Their role will be further explained in the next section 1.3..

1.3. KAR interacting proteins

The use of structural and biophysical studies has shed light on a growing appreciation that iGluRs do not assemble or operate in isolation, but instead represent one component of macromolecular complexes (Contractor *et al.,* 2011). Thus, like many other receptors and channels, KARs can interact with a whole set of interacting proteins. Each one of these

interacting proteins has been demonstrated to be relevant to neuronal KAR function through two main actions: 1) regulation of receptor trafficking to and from the neuronal and synaptic membrane and 2) modification of channel gating. KAR subunits interact with these interacting proteins through their CTD (Fièvre *et al.,* 2016; Lerma & Marques, 2013). The identification of these interacting proteins has improved the understanding on how KARs function and provided insight into the discrepancies between native and recombinant KAR properties (Lerma & Marques, 2013). Some examples of interacting proteins are described below.

NETO1 and NETO2

Previously mentioned KARs auxiliary subunits NETO1 and NETO2 exert an important influence on the function of KARs by radically altering their gating and pharmacological properties (thus, they have an effect both on channel gating and on current amplitudes). In recombinant systems, the co-expression of NETO1 and/or NETO2 with KARs alters the gating properties of these receptors. The most obvious impact of NETO is in the onset of the desensitization of kainate-evoked responses, which decelerates, while recovery from the desensitized state accelerates, resulting in a KAR steady current for longer periods in the presence of an agonist. Moreover, the rapid deactivation of kainate-induced currents upon agonist removal is also decelerated in the presence of NETO, suggesting an increase in the steady-state affinity of KARs when associated to NETO (Lerma & Marques, 2013). In the hippocampus, NETO1 contributes to postsynaptic KARs at mf-CA3 synapses, but the effect of NETO proteins on KAR targeting is still unclear (Carta *et al.* 2014; Lerma & Marques, 2013).

N-cadherin

N-cadherin participates in trans-synaptic complexes to ensure the adhesion between synaptic membranes and to organize the underlying multiprotein complex. In transfected heterologous cell lines, the activation of N-cadherins by ligand-covered latex beads was shown to recruit GluK2 to N-cadherin/b-catenin complexes. These cadherin/catenin complexes have an important role in the stabilization of kainate receptors at the synaptic membrane during synapse formation and remodelling (Coussen *et al*., 2002). Additionally, it was demonstrated that the faithful rescue of KAR segregation at mf-CA3 synapses critically depends on the amount of GluK2a and on a sequence in the GluK2a CTD (responsible for interaction with N-cadherin). Thus, targeted deletion of N-cadherin in CA3 pyramidal cells (PCs) greatly reduces KAR content in thorny excrescences (TE) and kainate receptor-mediated excitatory postsynaptic currents (KAR-EPSCs) at mf-CA3 synapses (Fièvre *et al.,* 2016).

C1q-like proteins: C1ql2 and C1ql3

Mf-derived C1ql2 and C1ql3 (C1q-like proteins, related to the C1q complement component) recruit functional postsynaptic KAR complexes, including NETO1 and KAR subunits to the CA3 pyramidal neurons, serving as extracellular organizers. C1ql2 and C1ql3 specifically bind the ATD of postsynaptic GluK2 and GluK4 KARs and the presynaptic Nrx3+SS5^{25b} (presynaptic neurexin 3 isoform that contains a specific sequence encoded by exon25b in splice site 5). Since C1q-like proteins are expressed in multiple brain regions, it was proposed that they could be involved in recruitment and functional control of KARs at a broad variety of synapses. Thus, C1q-like proteins seem to impact directly on glutamatergic circuit formation and function, illustrating a novel, and possibly general, principle of iGluR regulation (Matsuda *et al.,* 2016).

1.4. Physiological roles of KARs

Following the cloning of KAR subunits, depicting all the physiological roles that these receptors fulfil in the mammalian nervous system has been both elusive and more complex than previously imagined (Contractor *et al.,* 2011). Recent data show that the physiological roles of KARs can be summed up as: regulation of presynaptic function, postsynaptic neurotransmission, neuronal excitability and participation in long-term potentiation (LTP). They are implicated in processes ranging from neuronal development and differentiation to neurodegeneration and neuronal cell death (Contractor *et al*., 2011; González-González *et al*., 2012). The variety of these roles rely on their diverse: a) cellular expression, b) subcellular localization and c) signalling mechanisms (Carta *et al.,* 2014; Lerma & Marques, 2013), as will be further explored in this section. Taking this into account, it is easy to understand why the dysfunction of KARs has been implicated in several neurological disorders such as epilepsy, schizophrenia, depression and bipolar disorder (Møllerud *et al.,* 2016).

1.4.1. Diverse cellular expression

KARs are known to be highly expressed in the central nervous system (CNS) (Jane *et al*., 2009), however, the absence of specific antibodies against each receptor subunit has significantly hampered the exploring of their distribution. Thus, most of the information regarding their tissue expression comes from *in situ* hybridization studies. Until now, what it is known about cellular expression of each subunit of KARs can be summed up as follows:

a. GluK1 is mainly present in hippocampal and cortical interneurons, as well as in Purkinje cells and sensory neurons;
b. GluK2 is mostly expressed by principal cells (hippocampal pyramidal cells (CA1, CA3); both hippocampal and cerebellar granule cells; cortical pyramidal cells);

c. GluK3 is poorly expressed, appearing in layer VI of the neocortex and dentate gyrus (DG) in the hippocampus (it exhibits punctate labelling in the *stratum oriens* and *stratum radiatum*);
d. GluK4 is mainly expressed in neocortex, Purkinje cells and CA3 pyramidal neurons (it has a weaker expression in CA1 and DG);
e. GluK5 is expressed abundantly in the brain, being the most abundantly expressed subunit in hippocampus, present in all subregions, mainly in the principal cell layers (Carta *et al.,* 2014; Lerma & Marques, 2013).

GluK2/GluK5 receptors constitute the major population of KARs in the brain: both subunits are abundantly co-expressed in the cerebellum, neocortex, striatum, amygdala, and hippocampus, at higher levels than other KAR subunits (Bureau *et al*., 1999). In co-expressing cells, they form GluK2/GluK5 heterotetramers with a 2:2 stoichiometry (Reiner *et al*., 2012) exhibiting distinct functional and pharmacological properties, which differ significantly from the more studied GluK2 homotetramer (Barberis *et al*., 2008; Paramo *et al*., 2017). Interestingly, GluK2 has been described to be important for surface expression of other KAR subunits. Specifically, GluK5 subunit possesses an endoplasmic reticulum retention signal in the C-terminal domain, which prevents its cell surface expression. This retention signal is masked if GluK5 is co-expressed with GluK1, 2 or 3, allowing cell surface expression of these heteromeric assemblies (Gallyas *et al*., 2003; Jane *et al*., 2009; Ren *et al*., 2003). Regarding the specific abundance of heteromeric GluK2/GluK5 receptors, there is also a preferential assembly of the GluK2 and GluK5 ATD dimers and additional mechanisms which appear to work together to control the assembly of this specific complex (Reiner *et al*., 2012). Thus, GluK2 is one of the main subunits that drives GluK5 to the plasma membrane and to synaptic sites (Ruiz *et al*., 2005).

1.4.2. Diverse subcellular localization

It is currently known that KARs subcellular localization is highly regulated by the association with interacting proteins (as previously discussed in section 1.3.) and that these receptors can be located either in postsynaptic or presynaptic compartments.

On CA3 pyramidal neurons, KAR-EPSCs are only detected at mossy fiber inputs, at TEs, and are absent from the A/C fibers and performant path inputs (Fièvre *et al*., 2016). On the other hand, in physiological conditions, dentate granule cells (DGCs) use KARs specifically as presynaptic regulators of neurotransmitter release or axonal excitability at MF terminals and exclude them from postsynaptic densities. Presynaptic KARs facilitate glutamate release from mossy fiber terminals and contribute to the marked frequency-dependent short-term potentiation of glutamate release at mf-CA3 synapses.

1.4.3. Diverse signalling mechanisms

Despite the fact that KARs are iGluRs and share many common features with other glutamate iGluRs families, there is evidence that KARs can operate in two distinct modes: by a well characterized ionotropic action (canonical) and by an unconventional metabotropic mechanism (non-canonical).

Ionotropic signalling

Similarly to other ionotropic glutamate receptors, the ionic current of KARs is largely carried by Na^+. However, comparing with AMPARs, synaptic KARs mediate smaller amplitude currents with much slower decay kinetics, as a result of specific gating features (stabilization of partially bound open states) (Barberis *et al.,* 2008) and their interaction with auxiliary subunits (Lerma & Marques, 2013).

a. KARs gating

The use of crystallographic and spectroscopic techniques to depict iGluRs structure has allowed a profound understating of conformation changes underlying receptor function. Currently, there are highly detailed and testable physical models that can be correlated with kinetic data and mutagenesis-based structure-function studies. Additionally, these structural studies have also allowed a deeper understanding of the unusual dependence of KAR gating on extracellular cations and anions. In the absence of ion binding to defined sites on dimer interfaces, KARs accumulate in an unresponsive state analogous to fully desensitized receptors, and that loss of function in the absence of ions does not depend on agonist binding (Bowie 2010; Paternain *et al.*, 2003; Wong *et al*., 2006). So, this cation occupancy is the central requirement in keeping agonist-bound KARs in the activated state and out of desensitization. Deactivation is observed when the ligand unbinds from cation-bound states, whereas desensitization proceeds when the ligand is bound to cation-unbound states. Thus, the requirement for ion binding can render KAR activation sensitive to fluctuations in extracellular ion concentrations, which are thought to occur during periods of high neuronal activity (Contractor *et al.,* 2011). Altogether, this has led to the notion that, unlike AMPA receptors, KARs can respond differently according to different extracellular ion concentrations to regulate local excitability (Copits & Swanson 2012). This unique property of KARs may provide clues as to how subunit composition and/or auxiliary proteins might affect native receptors at glutamatergic synapses (Dawe *et al*., 2013). In sum, KARs can undergo either desensitization or deactivation. As an overall definition, desensitization will be defined as a decrease in the receptor-mediated biological response in the continued presence of or due to repeated exposure to an agonist and, on the other hand, deactivation will

be defined as a reduction in the receptor-mediated biological response after the removal of an agonist (Copits & Swanson, 2012).

b. KAR-EPSCs

KARs have an important role in excitatory signal transduction. Fig. 2 (top image) shows sample traces from EPSCs recordings at mf–CA3 synapse, which show a mixed AMPA and kainate receptor-mediated excitatory postsynaptic current (AMPA+KAR EPSCs; black). This AMPA+KAR EPSC is predominantly mediated by AMPA receptors, and the low-amplitude pharmacologically isolated KAR-EPSC (grey) has a small contribution in it. The peak-scaled KAR-EPSC (red) illustrates the relatively slow kinetics of KARs. Moreover, Fig. 2 (bottom image) shows that KAR-EPSCs sum effectively during high-frequency trains of activation.

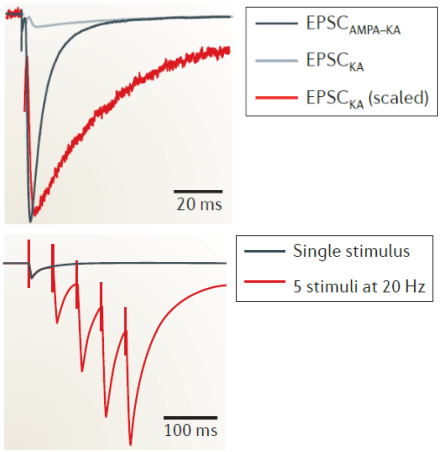

Figure 2 | Top image: Synaptic KARs mediate smaller amplitude currents with much slower kinetics than AMPA receptors. **Bottom image:** Repetitive activation of pharmacologically isolated mossy fiber KARs results in KAR-EPSC summation and increases the total charge transferred during the synaptic currents (Adapted from Copits and Swanson, 2012).

Metabotropic signalling

The metabotropic actions triggered by KARs have been described in different cell types and regions of the CNS. These actions are mainly associated either with the presynaptic control of neurotransmitter release or the postsynaptic regulation of neuronal excitability (Garand *et al.*, 2019; Lerma & Marques, 2013).

Metabotropic signaling of KARs was firstly noticed through the KAR-mediated modulation of GABA release, which did not require KAR ionotropic signalling, but was prevented by inhibition of G-protein and protein kinase C (PKC) activity (Rodríguez-Moreno & Lerma, 1998). Subsequently, it was also shown that a metabotropic signaling mediated a KAR-dependent inhibition of the slow after-hyperpolarizing potential (sAHP) caused by the postspike potassium current I (I_{sAHP}), enhancing neuronal excitability (Melyan *et al.*, 2002; Ruiz *et al.*, 2005). Recently, it was also shown that metabotropic KAR signaling is involved in the regulation of AMPAR trafficking, spine morphology and NMDAR-independent LTP (Petrovic *et al.*, 2017). Interestingly, the structural plasticity induced by KA was shown to be dependent on GluK2-containing KARs metabotropic signaling. However, the identity of the KAR subunit conferring metabotropic action is still unclear, once the literature is contradictory and no KAR subunits contain conventional G-protein binding motifs. Nevertheless, it is now generally accepted that

metabotropic KAR signaling is sensitive to pertussis toxin (PTX) and thus involves Go- rather than Gq-protein activation (Petrovic *et al*., 2017).

Regarding the KAR-mediated modulation of GABA release described at the beginning of the last paragraph, it has recently been demonstrated that independently activating either the ionotropic or metabotropic KAR signaling pathways produces a hyperpolarization of the reversal potential for GABA (E_{GABA}) (Garand *et al*., 2019). In this context, both ionotropic or metabotropic signalling modes of KARs may serve different functional roles for chloride homeostasis, allowing the cell to regulate the strength of GABAergic inhibition in response to excitatory activity in both a KCC2-dependent and KCC2 independent manner. The metabotropic signalling mode, which was shown to regulate E_{GABA} and is dependent on KCC2 transporter activity, places KARs on a growing list of proteins that are able to regulate KCC2 via G-protein signalling (Banke and Gegelashvili, 2008, Chorin *et al*. 2011, Mahadevan & Woodin, 2016). KCC2 interacts with the KAR subunit GluK2 and this physical interaction is required to maintain normal surface expression and oligomerization of the KCC2 protein (Garand *et al*., 2019; Mahadevan *et al*. 2014; Pressey *et al*. 2017). Thus, it is well known that disruptions in the Cl^- gradient are implicated in several neurological diseases and disorders that result from excessive glutamatergic excitation, including epilepsy and neuropathic pain (Coull *et al*. 2003, Kahle *et al*. 2014), marking metabotropic regulation of KCC2 as a potential target for the treatment of these diseases (Garand *et al*., 2019).

1.5. KARs distribution at mf-CA3 PC synapses

Most knowledge of the molecular and functional properties of KARs come from their study in the hippocampus. The main entry site of the hippocampus trisynaptic circuit is the perforant path, composed of axons originating from lateral and medial entorhinal cortex (EC) and contacting the outer and medial molecular layer of the dentate gyrus (DG), respectively. Granule neurons of the DG project MFs to Cornu ammonis (CA) 3 pyramidal neurons, which, in turn, project Schaffer collaterals to CA1 pyramidal neurons. Other inputs to granule neurons include interneurons located in the molecular layer and in the hilus of DG, principally composed of

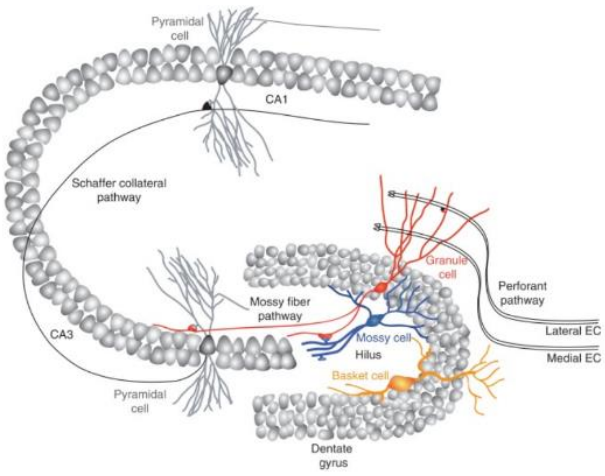

Figure 3 | Schematic view of hippocampal trysanaptic circuit, depicting the dentate gyrus, Cornus ammonis 3, and 1 pyramidal neurons (adapted from Bischofberger & Schinder, 2008).

basket and mossy cells (Fig. 3) (Bischofberger & Schinder, 2008).

CA3 pyramidal neurons receive three types of glutamatergic inputs, which are precisely positioned along apical and basal dendrites: from the EC (perforant path), from recurrent CA3 collaterals (associational/ commissural, A/C fibers) and from the DG through MFs. Glutamatergic synapses from these different inputs greatly vary in their structural and functional properties. MFs inputs make synaptic contacts on proximal dendrites of CA3 pyramidal cells in the *stratum lucidum* via MF giant boutons with multiple glutamate release sites (an average of 20 release sites) facing large postsynaptic structures called thorny excrescences (TEs) (Fig. 4, top image). In addition, MFs also make synaptic contacts with GABAergic interneurons through *en passant* boutons, as well as through filopodia emerging from mossy fibre terminals. In contrast, A/C and perforant path synapses are of the single site/single spine type (Rebola *et al*., 2017).

Mf-CA3 synapses display a wide dynamic range of short-term plasticity and express NMDA (N-methyl-D-aspartate) receptor-independent presynaptic forms of LTD and LTP. In CA3 PCs, stimulation of MF inputs but not of A/C inputs evokes EPSCs mediated by KARs (KAR-EPSCs), which contain the GluK2 subunit (Fièvre *et al*., 2015; Rebola *et al*., 2017).

At mf-CA3 PC synapses, KARs are present at both pre- and postsynaptic levels. At presynaptic level, KARs are thought to be composed of GluK2 and GluK3 subunits (Contractor *et al.,* 2001; Pinheiro *et al*., 2007). Presynaptic KARs are known to modulate glutamate release and to greatly influence the presynaptic plasticity at mf-CA3 synapses (Pinheiro *et al.,* 2013). Different mechanisms of presynaptic short-term facilitation driven by repeated stimulation of mf–CA3 PC synapses coexist. For instance, a tonic mode, known as frequency facilitation, occurs when mossy fibre firing switches from a tonic rate (<0.05 Hz) to a continuous firing rate up to several Hz (theta range frequency). On the other hand, a bursting mode is triggered by MF spike trains at frequencies from 10 Hz to 100 Hz. Both modes of presynaptic facilitation involve presynaptic KARs (Rebola *et al*., 2017). At a postsynaptic level, KARs are thought to be composed of GluK2, GluK4 and GluK5 subunits (Contractor *et al.,* 2003; Fernandes *et al.,* 2009; Mulle *et al.,* 1998; Pinheiro *et al.,* 2013), mediating

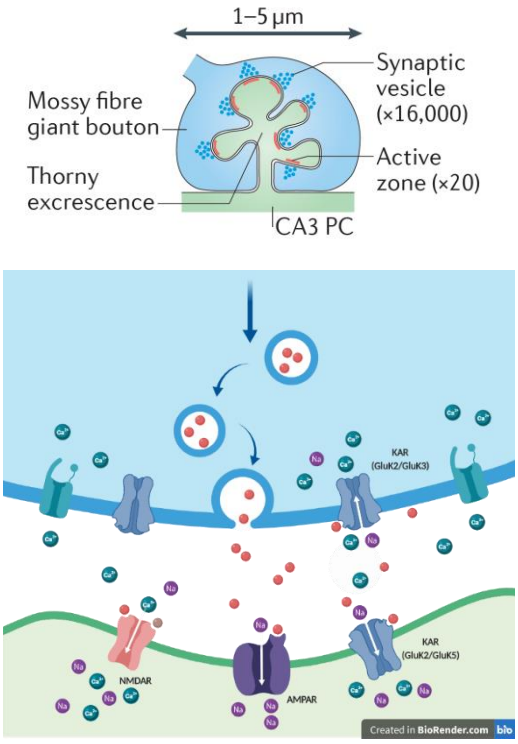

Figure 4 | Top image: Representative scheme of mf-CA3 pyramidal cell (PC) synapse in which mossy fiber form the so-called "giant bouton" and make contact with thorny excrescence (TE) (adapted from Rebola *et al*., 2017). **Bottom image:** Zoomed scheme showing the major key players in mf-CA3 PC synapse (designed in BioRender.com).

EPSCs of small amplitude (less than 10% of the total amplitude of mf-EPSCs, on average) and slow decay (Pinheiro *et al.*, 2007; Pinheiro *et al.,* 2013) (Fig. 4, bottom image). KARs also allow a temporal summation of synaptic signals transmitted by MFs (as described in 1.4.3.), being important for the synaptic integration and information transfer at these synapses (Pinheiro *et al.*, 2013). Interestingly, KAR driven EPSCs are subject to LTD that is dependent on the postsynaptic activation of PKC and calcium/ calmodulin-dependent protein kinase II (CaMKII) under conditions of presynaptic stimulation that also lead to LTP of NMDAR-EPSCs (Rebola *et al.*, 2017).

GluK2, GluK4 and GluK5 KARs subunits were identified as crucial components of these postsynaptic KARs in mf-CA3 synapses, through comparative analysis of KAR-EPSCs in knockout (KO) mice lacking one or more receptor subunits. Genetic removal of GluK2 eliminates KAR-EPSCs, demonstrating an obligatory role for this subunit in forming functional receptors at this synapse, as previously described. On the other hand, genetic ablation of GluK4 or GluK5 has a bidirectional effect on synaptic kinetics: either mice exhibit far slower kinetics (with KO of the GluK4 subunit) or exhibit more rapid current decay (KO of the GluK5 subunit). Elimination of both GluK4 and GluK5 in double knockout (DKO) mice exclude localization of KARs to mossy fiber postsynaptic sites but do not wholly prevent the expression of functional receptors in extrasynaptic domains (Copits & Swanson, 2012).

1.6. Pharmacology

1.6.1. Kainate: where does it come from?

Kainic acid or kainate (KA) (Fig. 5) is a potent neurotoxin firstly isolated from seaweed *Diginea simplex* (known as "kaininso" in Japanese) more than 50 years ago, and it was most known to cause amnesic shellfish poisoning. Later, its excitatory and neurotoxic actions were well established, and it was hypothesised that this compound would act on a specific subset of glutamate receptors (Watkins & Evans, 1981). Thus, this conformationally restricted glutamate analogue has become the prototypic agonist for KARs (Jane *et al.*, 2009), with a high-affinity binding to KAR subunits (K_D of 5-15 nM for GluK4 and GluK5; 70-100 nM for GluK1-3), as previously mentioned. Nowadays, this neurotoxin is known to induce neuropathological lesions and behavioral and electrophysiological acute seizures, reminiscent of those found in patients with mesial temporal lobe epilepsy (mTLE), through the activation of KARs (Crépel & Mulle, 2015).

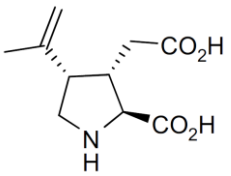

Figure 5 | Kainic acid.

1.6.2. KAR selective antagonists

A major concern in the development of subtype-selective KAR antagonists has resided in the lack of selectivity for KARs over AMPARs, once they exhibit overlapping sensitivities to most of compounds (Contractor *et al*., 2011; Jane *et al.,* 2009). For instance, CNQX and NBQX have been described as effective antagonists of AMPARs and KARs (Larsen & Bunch, 2011; Sheardown *et al*., 1990).

The likelihood of pharmacological heterogeneity in the KAR family is increased by the existence of splice variants and editing sites on some of the KAR subunits (Hollmann and Heinemann, 1994; Pinheiro & Mulle, 2006), as described in section 1.2.. Thus, unlike AMPARs, selective KARs agonists and antagonists have begun to emerge just two decades ago (Bleakman and Lodge, 1998; Brauner-Osborne *et al*., 2000; Jane *et al*., 2009; Kew & Kemp, 2005; Watkins & Jane, 2006).

Among all KAR subunits, the GluK1 has proved to be the most amenable subunit for the development of selective pharmacological agents, because of specific structural features of the binding site. Therefore, over the last two decades, subunit selective orthosteric agonists and antagonists for GluK1 subunit have been developed.

Structure–activity relationship (SAR) studies focused on changing the substituent at the 5-position of the uracil ring of the natural product willardiine (e.g. 5-iodowillardiine (Fig. 6)), lead to the development of GluK1 selective KAR agonists. On the other hand, antagonists have been developed by adding substituents to the N3 position of the uracil ring of willardiine (e.g. ACET (Fig. 6)) (Jane *et al.,* 2009). Hence, the discovery of these selective compounds for GluK1 containing KARs has shed light on the development of novel strategies for alleviating pathological pain, once these receptors modulate transmission in peripheral and central nociceptive pathways (Contractor *et al.,* 2011; Crépel & Mulle, 2015; Jane *et al.,* 2009). These selective GluK1 antagonists are also useful tools for investigating the role of GluK1-containing KAR subtypes in epileptic conditions.

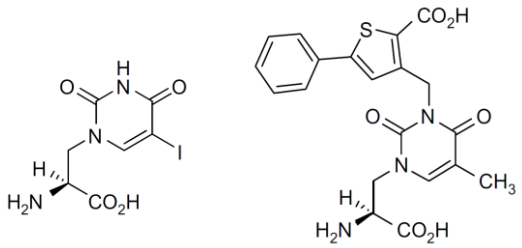

Figure 6 | Chemical structures of GluK1 agonists and antagonists. Abbreviations: 5-iodowilardiine, (S)-1-(2-amino-2-carboxyethyl)-5-iodopyrimidine-2,4-dione; ACET, (S)-1-(2-amino-2-carboxyethyl)-3-(2-carboxy-5-phenylthiophene-3-yl-methyl)-5-methylpyrimidine-2,4-dione.

Together with last compounds, and also based on willardiine structure, the University of Bristol Pharmaceuticals (UBP) series has further explored the functions of KARs in the CNS (Jane *et al.,* 2009). For instance, the 5-methyl derivative (S)-1-(2-amino-2-carboxyethyl)-3-(2-carboxythiophene-3-ylmethyl)-5-methylpyrimidine-2,4-dione (UBP310) (Fig. 8A) and (S)-1-(2-Amino-2-carboxyethyl)-3-(2-carboxybenzyl)pyrimidine-2,4-dione (UBP302) were used to obtain

the first X-ray crystal structures of the antagonist-bound form of the ligand binding core dimer of GluK1 (Mayer *et al*., 2006).

Although heteromeric GluK2/GluK5 KARs represent the most abundant population of KARs in the hippocampus and more generally in the brain (Carta *et al*., 2014), as described in section 1.4.1., no selective antagonist for this KAR subtype is available to date.

1.6.3. KARs allosteric modulators

Alternative strategies for targeting KAR receptors may include the development of positive or negative allosteric modulators or compounds that alter receptor association with functionally important auxiliary proteins, such as NETO1/2 (Contractor *et al*., 2011). Multiple allosteric-binding sites for small-molecule positive and negative modulators, ions, and polyamines as well as toxins have been identified in the NTD, LBD, and TMD of iGluRs (Zhu and Gouaux, 2017). The AMPAR LBD dimer interface harbours a binding site for several classes of positive allosteric modulators. However, much less is known about allosteric modulation of KARs. Concanavalin A and a few other plant lectins have been identified as positive allosteric modulators. Additionally, sodium and chloride ions are required in the extracellular medium for proper KAR activation and function (Bowie, 2002; Paternain *et al*., 2003; Wong *et al*., 2006), being important for channel gating and for stabilization of the LBD dimer interface (Jane *et al*., 2009).

Metal ions such as zinc (Fukushima *et al*., 2003; Huettner *et al*., 1998), lanthanum and gadolinium have been shown to inhibit KAR function (Jane *et al*., 2009). Conversely, zinc ions were found to have a unique potentiating effect selective for the KAR subunit GluK3 upon binding to the LBD dimer interface (Veran *et al*., 2012).

1.6.4. Important considerations

When developing new KAR ligands, it is important to always consider whether the experiments are being conducted on native or recombinant KARs. Testing new compounds on recombinant KARs may have different effects than testing the same compounds on native KARs, mainly due to the presence of interacting proteins in a living animal. Plus, in recombinant systems, it is important to guarantee that the recombinant receptor targeted exist as a native receptor, such as GluK2/GluK5 KARs. Then, comparison between studies and reproducibility of data should be made with caution for the following reasons: (1) receptor expression levels (whether recombinant or native KARs), and thus receptor reserve, are likely to vary in different laboratories; (2) in native KARs, animal species differences may occur (even a single change in the amino acid sequence of KARs subunits may lead to differences in pharmacology); (3) extracellular glutamate concentrations may vary from experiment to experiment (thus affecting receptor occupancy prior to addition of exogenous agents (having a most notable effect for

competitive orthosteric agonists or antagonists)); (4) KARs undergo rapid desensitisation and concanavalin A has been used in some laboratories to reduce this problem and this may alter KAR pharmacology (Jane *et al*., 2009). In experiments with recombinant KARs, this last issue may be solved using fast glutamate application systems.

2. EPILEPSY: AN OVERVIEW

2.1. Brief description, major clinical symptoms and general classification

Epilepsy is a term used to describe a spectrum of neurological disorders characterised by a lasting predisposition to generate spontaneous epileptic seizures, having numerous neurobiological, cognitive, and psychosocial consequences (Fisher *et al.*, 2014). Nevertheless, the occurrence of epileptic seizures *per se* does not necessarily imply a diagnosis of epilepsy, once they can also occur as isolated events not associated with an enduring predisposition.

Nowadays, epilepsy is known to affect over 70 million people worldwide and its incidence is bimodally distributed with the highest risk in infants (less than 1 year old) and older age groups (over 50 years old) (Thijs *et al.*, 2019), being a cause of substantial morbidity and mortality. Patients can experience several forms of manifestations including seizures in addition to other signs, symptoms and features that define a specific phenotype (Blair, 2012). Seizures result from aberrant, excessive and synchronous firings of groups of neurons within the brain, leading to alterations in consciousness, sensation and behavior. These seizures can originate from within a specific brain region, being classified as focal or localization-related seizures, or they can occur simultaneously within both hemispheres of the brain, being classified as generalized seizures (Hauser *et al.,* 2017).

The epilepsy classification has undergone several changes over the years (Blair, 2012) and the International League Against Epilepsy (ILAE) has been taking a leading role in the establishment of seizure and epilepsy classification systems, being the largest academic body in epilepsy community (Chang *et al.* 2017). According to ILAE, the new Classification of Epilepsies (stated in 2017) should be established through a multilevel classification based on seizure type, epilepsy type and epilepsy syndrome. Additionally, the etiology of the patient's epilepsy should always be considered (Scheffer *et al.*, 2017).

2.2. Therapeutic approaches

Seizures can be reduced in many epileptic patients through treatment with anti-epileptic drugs (AEDs) which dampen brain excitability by boosting inhibitory or attenuating excitatory neurotransmission. AEDs either enhance GABAergic synaptic inhibition, modulate voltage-gated sodium and calcium channels, impact synaptic release or attenuate glutamate receptor function (Mulle & Vincent, 2009; Rogawski & Loscher, 2004). There are more than 25 AEDs in common use nowadays and the choice of antiseizure medication should consider the seizure type, epilepsy syndrome, comorbidities, tolerability risks, and individual characteristics. Among AEDs for focal

and most generalised seizures are benzodiazepines, lamotrigine, levetiracetam, perampanel, phenobarbital, topiramate, sodium valproate and zonisamide. Regarding focal seizures only, available AEDs are brivaracetam, carbamazepine, eslicarbazepine acetate, gabapentin, lacosamide, oxcarbazepine, phenytoin, pregabalin, tiagabine and vigabatrin. The seizure remission is likely to reduce morbidity and to decrease the risk of premature mortality associated with continuing seizures, particularly convulsions (Devinsky et al., 2015; Neligan *et al.*, 2012; Thijs *et al.*, 2019). For most patients, AEDs prevent seizures, interfere with epileptogenesis, and eliminate brain damage produced by seizures. However, many AEDs fail to control seizures and/or have deleterious side effects in some patients. These side effects may include dizziness, drowsiness, gastrointestinal disturbances (nausea, diarrhoea or constipation), tiredness and others.

There are no current pharmacological approaches capable of modifying the progression of the disease neither to prevent it at risky patients (Hauser *et al.,* 2017; Kwan & Brodie, 2000; Thijs *et al.*, 2019). Nowadays, surgical procedures as stimulation of vagus nerve, responsive neurostimulation, or surgical resection of the epileptic tissue, are the remaining alternative clinical approaches to alleviate these patients' symptomatology. There is an urgent need of identifying new compounds that could selectively target pathogenic pathways without disturbing normal brain functions (Vincent & Mulle, 2009), in order to be effective and decreasing the amount of side effects.

2.3. Associated genetic determinants

About 50% of all human epilepsies have genetic determinants, with more than 70 genes known to be linked to an epileptic phenotype. Epilepsy genetics can be grouped into two main broad categories: monogenic epilepsies, in which a single variant of large effect is considered causative, and complex genetic epilepsies, in which a presumed combinatorial effect of multiple susceptibility variants is thought to underlie the disease (Symonds, 2017). Advances such as genome-wide association studies (GWAS), whole exome sequencing (WES), and whole genome sequencing (WGS) are beginning to uncover the genetic architecture of some of these epilepsies (Thijs *et al.*, 2019).

Regarding monogenic epilepsies, people with familial monogenic epilepsies represent a small percentage (5–10%) of all genetic epilepsies (Helbig and Lowenstein, 2013; Rein *et al.*, 2009). There are more than 30 different mutated genes in these families with rare autosomal dominant monogenic epilepsies with high penetrance. These mutations can be found in genes coding for ions channels, neuronal receptors, transcription factors and enzymes. On the other hand, in complex genetic epilepsies, the underlying causes of most of the cases of presumed genetic

generalised epilepsies are still unknown. The genetic cause of these common epilepsies is presumably complex, involving contributions from multiple genes (Thijs *et al*., 2019).

Focal epilepsies, such as temporal lobe epilepsy, which will be further explored in the next section, can also have a genetic basis. Mutations associated with focal epilepsies often involve genes in the mTOR pathway but can also involve voltage-gated (e.g. *SCN1A*) or ligand-gated channels (e.g. *GABRG2*) (Ricos *et al*., 2015; Scheffer *et al*. 2014; Weckhuysen *et al*. 2016). In summary, for these cases, there is probably a spectrum in the genetic contribution: from individuals in whom genetics are the primary cause through to those whose underlying genetic background predisposes them to the development of epilepsy after an acquired brain insult (Thijs *et al*., 2019).

Regarding KARs, there is little evidence for spontaneous mutations involving these receptors in epilepsy syndromes (at least linked to functional mutations affecting the structure of the receptor subunit(s)), both in human and mouse (Vincent & Mulle, 2009). Nevertheless, there has been an association of a polymorphism in the non-coding region of the human *GRIK1* gene (GluK1 KAR subunit) with juvenile absence epilepsy, a common subtype of idiopathic generalized epilepsy (Sander et al., 1997). Additionally, a significant linkage and association between *GRIK2* and autism have also been revealed in mouse, and epilepsy is known to be present in an estimated 30% of the autistic population (Vincent & Mulle, 2009). Despite the fact of lack of evidence for spontaneous mutations in KARs, there is increasing evidence about their role in epileptiform activity in temporal epilepsy, as it will be further explored in the next sections.

2.4. Temporal lobe epilepsy

2.4.1. Background and etiology of TLE

Temporal lobe epilepsy (TLE) is the most common acquired epilepsy, being also the most common form of focal or localization-related epilepsy. It is typically preceded by an inciting brain injury which leads to the transformation of a normal brain circuit into a hyperexcitable one, a process known as epileptogenesis (Gano *et al*. 2018; Lévesque *et al*., 2013). This brain injury may include febrile seizures, head trauma, brain malformations, infections (e.g. encephalitis and meningitis) and even some tumours within the temporal lobe (Lévesque *et al*., 2013). After this injury, epileptogenesis evolves during a latent period (a few months or years), followed by the chronic epileptic state (Hadera *et al*., 2015). Beyond debilitating seizures, common comorbidities of TLE include cognitive deficits, anxiety and depression (Hauser *et al.* 2017). There are also presumed genetic forms of TLE (Lévesque *et al*., 2013), as described in the previous section 2.3. for focal epilepsies, and recently, epigenetic mechanisms have also been linked to this pathology (Hauser *et al.,* 2017).

There are two main forms of TLE: the mesial temporal lobe epilepsy (mTLE), the most common form, which involves the medial or internal structures of the temporal lobe, and the neocortical temporal lobe epilepsy (nTLE), which involves the outer portion of the temporal lobe. mTLE usually originates in the hippocampus or its surrounding structures and is associated with hippocampal sclerosis.

2.4.2. The hippocampal trisynaptic circuit and its dysfunction in mTLE

Histological analysis of the resected tissue from mTLE patients or mTLE animal models reveals selective neuronal loss of pyramidal cells of the CA1, CA3 and neurons in hilus such as mossy cells. There is also a loss of a subpopulation of GABAergic interneurons and other small lesions can be observed in the amygdala and parahippocampal gyrus. Another important histological feature that may occur is the dispersion of DG granule cells, named granule cell dispersion (GCD). Along with the hippocampal sclerosis and GCD, an aberrant mossy fiber sprouting in the molecular layer of the DG is observed, resulting in a major network reorganization in the hippocampus. This phenomenon is called reactive plasticity (Artinian *et al.*, 2011; Lévesque *et al.*, 2013; Peret *et al.*, 2014).

While in a normal hippocampus, mossy cells provide glutamatergic inputs to the inner molecular layer of the DG, in the epileptic hippocampus with hippocampal sclerosis, the loss of hilar neurons leads to a deafferentation of the granule cells dendrites in the inner molecular layer. As a result, the surviving DG cells sprout axon collaterals and re-innervate empty synaptic sites with functional connections, resulting in an abnormal hippocampal circuitry. In other words, mossy fibers originating from DG cells - recurrent mossy fibers (rMFs) - form abnormal excitatory synapses onto other DG cells forming recurrent excitatory circuits (Fig. 7) (Chang & Lowenstein, 2003; Crépel & Mulle, 2015; Venceslas & Corinne, 2017). MFs not only sprout into the molecular layer (giving rise to supragranular MFs) but also within the CA3 *stratum oriens* region and into CA2 and CA1, giving rise to MFs onto pyramidal cells. However, the role of supragranular MFs are best studied as a potential epileptogenic mechanism.

KARs, which were explored in detail in section 1, are expressed and functional in principal neurons of CA1, DG and CA3, as well as in interneurons (Fièvre *et al.* 2016). In TLE, these recurrent MF inputs impinging on DG cells operate mostly via ectopic synaptic KARs (Epsztein *et al.* 2005). A

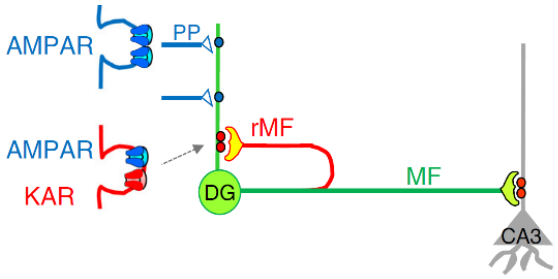

Figure 7 | Schematic drawing of recurrent MF-operated synapse contacting DGCs. These rMFs operate via ectopic KARs. PP: perforant path; MF: mossy fiber; AMPAR, glutamate receptors of the AMPA type (Adapted from Crépel & Mulle, 2015).

major finding at the basis of the project demonstrating a central role of these ectopic KARs in the generation of seizures will be described in section 2.4.5..

2.4.3. Available animal models

Over the last four decades, animal models that reproduce the electroencephalographic, behavioral and neuropathological features of TLE have been developed (Lévesque *et al.*, 2015). There are two main animal models of TLE and both use the focal or the systemic administration of a specific chemoconvulsant. Thus, one of these models uses kainic acid/kainate (a cyclic analog of L-glutamate, and an agonist of glutamatergic AMPA and KARs) and the other model uses pilocarpine (a cholinergic muscarinic agonist (i.e., M1 muscarinic receptors), activating also NMDA receptors for seizure maintenance). Both models induce an initial brain injury (status epilepticus) that is followed by a latent period and by the recurrence of spontaneous seizures originating from the temporal lobe. This process may take several months to evolve, after the initial status epilepticus (Lévesque *et al.*, 2015; Nirwan *et al.*, 2018; Vincent & Mulle, 2009).

Although these animal models do not exactly match complex etiologies and features identified in humans, they have been shedding light both on the understanding of TLE pathophysiology (since they reproduce the typical histopathological alterations and spontaneous chronic seizures seen in epileptic patients) and on the discovery of new AEDs (Lévesque *et al.*, 2015; Rogawski, 2006; Vincent & Mulle, 2009).

2.4.4. Current pharmacotherapies and clinical approaches

As previously mentioned, there are more than 25 AEDs currently available to control or to reduce seizure occurrence. In TLE, more than 30% of the patients are pharmacoresistant to available AEDs. The AEDs mainly act on voltage-gated sodium and calcium channels to selectively modify neuronal excitability or enhance GABAergic inhibition (Rogawski and Loscher, 2004) and, apart from that, they are known to provoke deleterious side effects. Thus, the surgical resection of the epileptic tissue is sometimes the only treatment option for these patients (Hauser *et al.,* 2017; Lévesque *et al.,* 2013). If surgery does not work or cannot be performed, devices such as vagus nerve stimulation or responsive neurostimulation might be a solution, as previously mentioned.

It is imperative to find novel therapeutic and clinically relevant approaches to improve patients' quality of life. Thus, identifying new compounds that could selectively target pathogenic pathways without disturbing normal brain functions would be very appropriate. Considering that ectopic synaptic KARs in the DGCs markedly contribute to epileptiform activity in animal models of TLE, it has been proposed that ectopic KARs represent a promising new therapeutic target

for TLE patients displaying pharmacoresistance (Vincent & Mulle, 2009). Thus, this new possible target will be further explored in the next section 2.4.5..

2.4.5. Ectopic KARs at rMF-DGCs synapses: contribution to TLE

The dentate gyrus plays a major role at the gate of the hippocampus, filtering incoming information from the medial and lateral entorhinal cortex. In physiologic conditions, DGCs display a sparse firing mode, behaving as coincidence detectors, due to the fast kinetics of excitatory synaptic events, restricting integration of afferent inputs to a narrow time window (Artinian *et al.,* 2011). Additionally, it is known that MF connections onto CA3 PCs are also sparse, and each CA3 PC is contacted on average by 50 DGCs representing a very low percentage of connectivity (Rebola *et al*., 2017).

Both in the hippocampus of human patients and in animal models of TLE, DGCs mossy fibers sprout to form aberrant glutamatergic excitatory synapses onto other DGCs, forming the so-called recurrent mossy fibers. Thus, in addition to fast AMPAR-mediated synaptic events, DGCs will also display slow postsynaptic KAR-mediated synaptic events originating from these rMF synapses (Crépel & Mulle 2015; Epsztein *et al*., 2005). These aberrant postsynaptic KARs in DGCs are mostly heteromeric GluK2/GluK5 receptors. Hence, these rMF synapses drastically impair the temporal precision of EPSP-spike coupling due to the selective interplay between aberrant rMF-mediated KAR-EPSCs and persistent sodium current (I_{NaP}). As a result, the change of the input–output relationship leads to an alteration of the coincidence detection operation and switches the firing pattern of DGCs from a sparse to a sustained regime (Artinian *et al.,* 2011). In an animal model of TLE (with pilocarpine-treated mice) it was observed that the lack of GluK2 does not affect the establishment of rMF connections, however, this subunit plays a major role in the epileptiform activity driven by rMFs in the DG (Peret *et al.,* 2014). Thus, it could be concluded that ectopic KARs containing GluK2 are involved in rMF network-driven bursts in DG and contribute to epileptiform activity in patients with TLE. However, despite all available data, the recruitment of the KARs at aberrant MF (rMF)-DG synapses is not fully understood. Understanding the molecular mechanisms responsible for the recruitment of KAR receptors at mf-CA3 synapses and how these receptors contributes for epileptic behavior may open up new possibilities to neutralize the aberrant KAR, attenuating epileptic seizures (Crépel & Mulle, 2015; Fièvre *et al*., 2016).

Considering all these aspects, GluK2/GluK5 KARs seem to be key players in originating recurrent seizures in TLE, by inducing hyperexcitability in DG neurons, placing them as potential therapeutic targets. As described, the main goal of this Master thesis will be to validate and characterize potential pharmacological compounds able to selectively target GluK2/GluK5 KARs, being them orthosteric antagonists or allosteric modulators.

3. TARGETING GLUK2/GLUK5 KARS IN TLE

3.1. Pharmacological tools targeting GluK2/GluK5 KARs: a historic overview

As previously described, about 30% TLE patients exhibit marked pharmacoresistance to current available AEDs on the market. There is an urgent need to find alternative and safer therapeutic options for pharmacoresistant TLE patients. In this context, the fact that KARs have mainly a modulatory role in synaptic transmission (contrary to NMDARs and AMPARs, which are known to be the major postsynaptic targets for synaptically released glutamate), as well as a role in the regulation of hippocampal networks, makes them potential therapeutic targets to downregulate hyperexcitable neuronal networks (Jane *et al.*, 2009).

As referred in the previous sections, until nowadays, no selective ligands for the other KAR subunits besides GluK1 have been identified, despite intense efforts over the last decades. Targeting KARs has become an even more promising therapeutic strategy following the studies which have clearly demonstrated that GluK2/GluK5 KARs ectopically expressed in DGCs play a major role in chronic and recurrent seizures in TLE. Taking this into account, the development of new pharmacological agents and strategies directly targeting and blocking these KARs might constitute a novel powerful group of AEDs. In this way, the inhibition of ectopic synaptic KARs in DGCs will likely put a break on the hyperexcitability of DG neuronal networks. Importantly, acting on these specific heteromeric KARs should spare hippocampal interneurons, which mostly express KARs containing the GluK1 subunit. Altogether, targeting aberrant GluK2/GluK5 KARs in DGCs might constitute a novel and promising anti-epileptic strategy since its blockade strongly reduces chronic and recurrent seizures without affecting the main AMPAR-mediated excitatory neurotransmission (Crépel & Mulle, 2015).

3.2. Development of GluK2/GluK5 antagonists

UBP310 (Fig. 8A) was originally developed as a GluK1-selective antagonist (Dolman *et al.*, 2007) and later found to also potently antagonize GluK3 (Perrais *et al.,* 2009). It was further demonstrated that UBP310 is also an antagonist of the recombinant and synaptic GluK2/GluK5 receptors (Pinheiro *et al.*, 2013). Interestingly, at postsynaptic sites of mf-CA3 synapses (which likely contain mostly GluK2/GluK5 KARs), UBP310 blocks these GluK2/GluK5 KARs and spares synaptic AMPARs and NMDARs (Pinheiro *et al.*, 2013). Additionally, UBP310 was also shown to spare presynaptic KARs, likely composed of GluK2/GluK3, not affecting hippocampal MF short-term plasticity (Perrais *et al.*, 2009). In mouse models of TLE, UBP310 has been shown to display antiepileptic efficacy (Peret *et al.*, 2014). Even though UBP310 is not selective to GluK2/GluK5

receptors, it might be very useful as a control compound during drug screening for new GluK2/GluK5 antagonists, as it will be further explored later in the results and discussion sections.

This Master thesis relied on a collaboration with the laboratory of Dr. Bernard Pirotte at the University of Liège in Belgium, who designed and synthesized new orthosteric GluK2/GluK5 KAR antagonists. The *N,N'*-disubstituted thymine derivative UBP310 was used as a model for the design of new orthosteric GluK2/GluK5 KAR antagonists. The rationale behind the design of these new orthosteric GluK2/GluK5 KAR antagonists considered that the amino acid moiety [$CH_2CH(NH_2)$ COOH] linked at the N1 position of the thymine nucleus (Fig. 8B) of UBP310 (Fig. 8A, shown in red dashed square) needed to be preserved, to guarantee selectivity for KA versus AMPA receptors and analogy with the natural ligand glutamate (Fig. 8C). On the other hand, the 2-carboxythien-3-ylmethyl moiety linked at the N3 position of the thymine nucleus of UBP310 (Fig. 8A, shown in green dashed circle) was modulated in order to design new KAR antagonists expected to show selectivity for the GluK2/GluK5-type receptors.

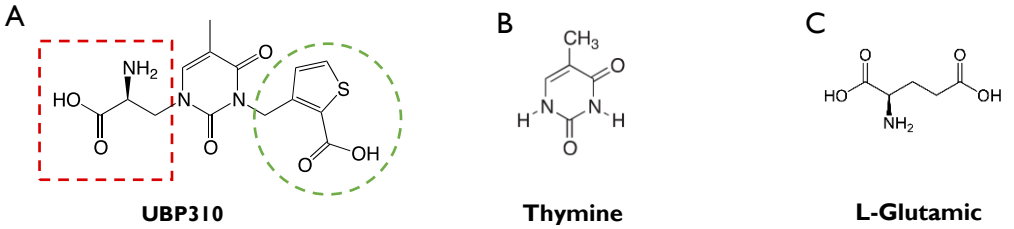

Figure 8 | A UBP310 reference molecule (red dashed square indicates the molecule moiety that was kept in order to guarantee the selectivity to KA versus AMPA receptors and also its similarity with the natural ligand glutamate, while the green dashed circle was the molecule moiety modified in order to design new KAR antagonists); **B** Thymine; **C** L-Glutamic acid.

Several modifications were explored in the chemical and structural formula of UBP310. Regarding the compounds tested in the scope of this Master thesis, we collectively explored the impact of the replacement of the thiophene ring (C4H4S) by another isosteric ring, namely:

a. A pyridine ring (C_5H_5N), with the introduction of a carboxylic function (**LC29** (Fig. 9A)) on this ring;
b. A benzene ring (C_6H_6), with the introduction of a nitro functional group (**LCKE10** (Fig. 9B)) or a carboxyl functional group (**P03** (Fig. 9C)) on this ring.

LC29 was synthesized in the form of trifluoroacetate (which was considered in the calculation of the molecular weight). It is soluble in water, but less soluble in DMSO and insoluble in organic solvents. LCKE10 and P03 were both co-crystallized with half a molecule of water (which was considered in the calculation of the molecular weight) and both are soluble in DMSO.

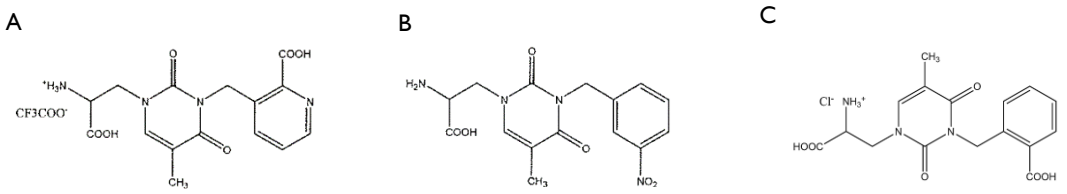

Figure 9 | GluK2/GluK5 potential orthosteric GluK2/GluK5 KARs antagonists.

All these new synthesized compounds were analysed by NMR spectroscopy and by elemental analysis, to warrant the structure conformity and the analytical purity (>95%). After a first phase of compounds screening, the ester prodrugs of the most interesting compounds will be synthesized and are expected to have a better probability to cross the blood brain barrier (BBB) (due to increased lipophilicity) and to reach the CNS, comparing to UBP310.

3.3. Development of GluK2/GluK5 KARs allosteric modulators

There are some known differences between AMPA and kainate receptors regarding amino acid residues at the level of the dimer interface of the LBD. The rationale behind developing new allosteric modulators of KARs takes into consideration the design of compounds able to interact with a histidine residue (His792) of these receptors in their allosteric binding site. At the same place at the level of the allosteric binding site, the AMPA receptor shows an aspartate residue.

Interestingly, ATM 2_21 (Fig. 10A) was found to cocrystallize with the GluK1 LBD but not with the GluA2 LBD (establishment of an ionic bridge between the carboxylic function of ATM 2_21 and His792). Surprisingly, ATM 2_32 (Fig. 10B) cocrystallizes with the GluA2 LBD, but not with the GluK1 LBD. Such a result could indicate that ATM 2_21 is a selective KAR positive allosteric modulator (PAM), while ATM 2_32 is a selective AMPAR PAM.

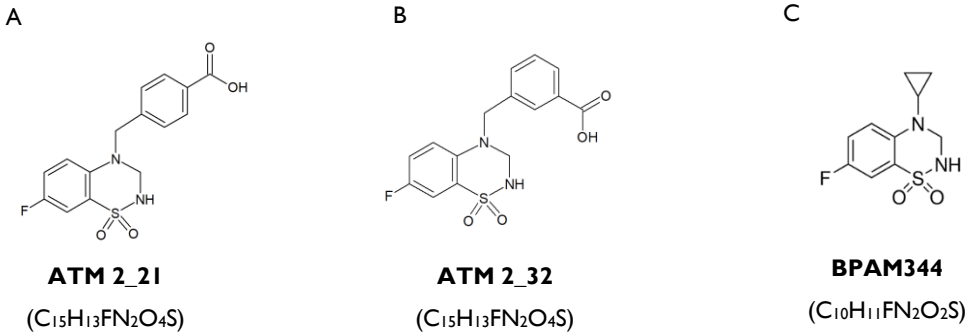

Figure 10 | GluK2/GluK5 putative positive allosteric modulators (PAMs).

4-cyclopropyl-7-fluoro-3,4-dihydro-2H-1,2,4-benzothiadiazine 1,1-dioxide (BPAM344 (Fig. 10C)) has been characterized as a promising positive allosteric modulator of KARs, capable of increasing their glutamate-evoked currents. Concretely, this compound was shown to potentiate glutamate-evoked currents of homomeric GluK2a 21-fold at 200 μM, with a half maximal effective concentration (EC_{50}) of 79 μM. At the same time, it was shown to decrease its desensitization kinetics and to have a minor effect on their deactivation kinetics. Additionally to GluK2a, BPAM344 also potentiated the peak current amplitude of KAR subunits GluK3a, GluK1b and AMPA subunit GluA1i. This should be taken into consideration during drug screenings. Despite the potency of the modulator, BPAM344 may prove to be a useful pharmacological tool to slow the entry into the desensitized state of fast desensitizing KARs for identification of orthosteric ligands (e.g., agonists or partial agonists) as well as functional studies *in vivo*. However, it remains to be determined whether these compounds are also effective on native KARs, as well if KAR-positive allosteric modulators may improve cognitive functions (Larsen, 2017).

3.4. Silencing GluK2 subunit as a therapeutic approach in TLE

The use of GluK2 knockout mice (GluK2 -/-) has clearly demonstrated that acute seizures are induced *in vivo* by systemic administration of low doses of KA, as well as excitotoxic cell death depend on GluK2-containing KARs, whereas higher doses may also implicate activation of AMPARs (Crépel & Mulle, 2015). Additionally, it was shown in animal models of TLE a strong reduction of both interictal and ictal activities in the DG recorded *in vitro* and *in vivo* in GluK2-/- mice. Therefore, it was demonstrated that aberrant GluK2-containing KARs at rMF synapses play a major role in chronic seizures in TLE (Peret *et al.,* 2014).

This opened up the possibility of targeting GluK2 subunit as a robust therapeutic approach in TLE. Silencing this subunit in DG of TLE animal models, which express aberrant KARs in rMF-DG synapses, might be a powerful therapeutic approach to be explored.

3.5. Master thesis hypothesis and main goals

Currently available pharmacotherapies for TLE are focused in controlling the disease symptomatology, acting both on inhibitory and excitatory signalling. However, thirty percent of TLE patients are refractory to these therapies, having recurring epileptic seizures over time. Thus, it is urgent to find novel therapeutic and clinically relevant approaches. The main hypothesis of this Master thesis considers that ectopic synaptic KARs in the DGCs markedly contribute to epileptiform activity, thus, blocking their activity may represent a promising new therapeutic approach for TLE patients displaying pharmacoresistance, alleviating their disease-related symptomatology.

This project aims to validate and characterize new putative orthosteric antagonists (LCKE10, LC29, P03) or allosteric modulators (ATM 2_21, ATM 2_32 and BPAM344) on GluK2/GluK5 KARs using slice electrophysiology. The full set of experiments was done in a synaptic context (mf-CA3 synapses) on native KARs, applying different electrophysiology protocols. The potential new pharmacological compounds may represent additional options for novel anti-epileptic drugs (AEDs), mainly for TLE.

II. MATERIALS AND METHODS

1. MICE AND ETHICAL CONSIDERATIONS

The animals used in this study were C57BL6/J wild type (WT) mice, from P20 to P26, with a balanced number of males and females. The mice were provided with food and beverage *ad libitum* and were placed in cages with adequate bedding. All experimental procedures related to the use of mice, including animal anesthesia and euthanasia procedures, were performed in accordance with the European Union (EU) guidelines (directive 2010/63/UE) and under the authorization of the 'EOPS' (Exempt d'Organisme Pathogène Spécifique) of the *Institut Interdisciplinaire de Neurosciences* (IINS).

2. DRUGS

The following drugs were used in patch-clamp experiments: bicuculline (Hello Bio®), D-AP5 (Hello Bio®) and LY303070 (ABX®). As experimental drugs, the ones tested were: UBP310, LCKE10, LC29, P03, BPAM344, ATM 2_21 and ATM2_32. Apart from UBP310 (Hello Bio®), all experimental drugs were supplied by Dr. Bernard Pirotte's laboratory in Liège, Belgium. Aliquots of stock solutions were prepared and frozen at -20°C.

The experimental drugs were categorized into two main different groups: KAR putative orthosteric antagonists (UBP310, LCKE10, LC29 and P03) and KAR putative allosteric modulators (BPAM344, ATM 2_21 and ATM2_32). The molecular weight (M = $g.mol^{-1}$) was calculated both for KAR putative orthosteric antagonists (Fig. 1) and KAR putative allosteric modulators (Fig. 2), according to each chemical structure. After it, a stock solution was prepared considering the mass (mg) available of each pharmacological compound. Thus, for each pharmacological compound tested, it was prepared an initial stock solution in filtered dimethyl sulfoxide (DMSO) or DMSO and ultra-pure water, depending on each molecular weight, mass and compound solubility. Stock solutions with molar concentrations of 5 mM, 10 mM, 20 mM or 100 mM have been prepared.

KAR putative orthosteric antagonists

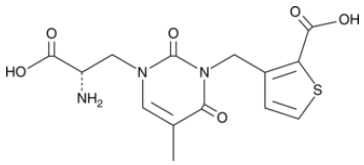

UBP310 ($C_{14}H_{15}N_3O_6S$)

MW ≈ 353,35 g.mol^{-1}

m = 10 mg

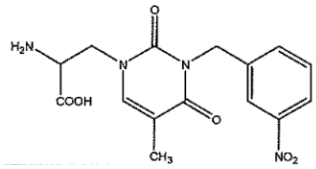

LCKE10

($C_{15}H_{16}N_4O_6 \cdot ½\ H_2O$)

MW ≈ 357,28 g.mol^{-1}

m = 30 mg

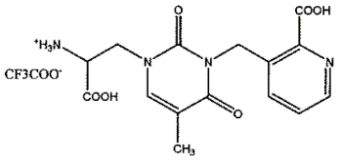

LC29

($C_{15}H_{17}N_4O_6\ CF_3COO^-$)

MW ≈ 462,29 g.mol^{-1}

m = 20 mg

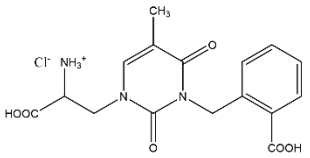

P03

($C_{16}H_{17}N_3O_6\ HCl^- \cdot ½H_2O$)

MW ≈ 392,76 g.mol^{-1}

m = 200 mg

Figure 1 | KAR putative orthosteric antagonists. Representation of each structural formula, molecular formula, molecular weight (MW) and mass (mg).

KAR putative allosteric modulators

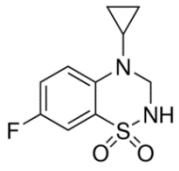

BPAM344

($C_{10}H_{11}FN_2O_2S$)

MW ≈ 242,27 g.mol^{-1}

m = 5,14 mg

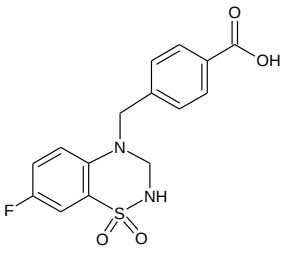

ATM 2_21

($C_{15}H_{13}FN_2O_4S$)

MW ≈ 336,32 g.mol^{-1}

m = 5,27 mg

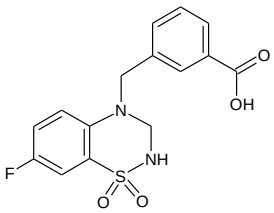

ATM 2_32

($C_{15}H_{13}FN_2O_4S$)

MW ≈ 336,32 g.mol^{-1}

m = 5,01 mg

Figure 2 | KAR putative allosteric modulators. Representation of each structural formula, molecular formula, molecular weight (MW) and mass (mg).

Stock solutions preparation of KAR putative orthosteric antagonists

UBP310: C_{stock} = 10 mM; solvent: DMSO

353,35 g ----- 1 mol
0,010 g ----- x mol x = 2,83 x 10^{-5} mol
$M = \frac{n}{V} \Leftrightarrow 10 \times 10^{-3} = \frac{(2{,}83 \times 10^{-5})}{V} \Leftrightarrow V = 0{,}00283\ L = 2{,}83\ mL$ of DMSO

LCKE10: C_{stock} = 20 mM; solvent: DMSO

357,2833 g ----- 1 mol
0,030 g ----- x mol x = 8,3967 x 10^{-5} mol
$M = \frac{n}{V} \Leftrightarrow 20 \times 10^{-3} = \frac{(8{,}3967 \times 10^{-5})}{V} \Leftrightarrow V = 0{,}00419835\ L = 4{,}20\ mL$ of DMSO

LC29: C_{stock} = 5 mM; solvent: DMSO, water and drops of trifluoroacetic acid

462,290 g ----- 1 mol
0,020 g ----- x mol x = 4,3263 x 10^{-5} mol
$M = \frac{n}{V} \Leftrightarrow 5 \times 10^{-3} = \frac{(4{,}3263 \times 10^{-5})}{V} \Leftrightarrow V = 0{,}0086526\ L = 8{,}65\ mL$ of DMSO and water

P03: C_{stock} = 100 mM; solvent: DMSO

392,75616 g ------ 1 mol
0,2 g ------ x mol x = 5,092 x 10^{-4} mol
$M = \frac{n}{V} \Leftrightarrow 100 \times 10^{-3} = \frac{(5{,}092 \times 10^{-4})}{V} \Leftrightarrow V = 0{,}005092\ L = 5{,}09\ mL$ of DMSO

Stock solutions preparation of KAR putative allosteric modulators

BPAM344, ATM 2_21 and ATM 2_32: C_{stock} = 10 mM; solvent: DMSO

BPAM344:
242,27 g ---- 1 mol
0,00514 g ---- x mol x = 2,122 x 10^{-5} mol
$M = \frac{n}{V} \Leftrightarrow 10 \times 10^{-3} = \frac{(2{,}122 \times 10^{-5})}{V} \Leftrightarrow V = 0{,}002122\ L = 2{,}12\ mL$ of DMSO

ATM 2_21:
336,3165232 g ---- 1 mol
0,00527 g ---- x mol x = 1,5670 x 10^{-5} mol
$M = \frac{n}{V} \Leftrightarrow 10 \times 10^{-3} = \frac{(1{,}5670 \times 10^{-5})}{V} \Leftrightarrow V = 0{,}001567\ L = 1{,}57\ mL$ of DMSO

ATM 2_32:
336,3165232 g ------ 1 mol
0,00501 g ------ x mol x = 1,4896681 x 10^{-5} mol
$M = \frac{n}{V} \Leftrightarrow 10 \times 10^{-3} = \frac{(1{,}4897 \times 10^{-5})}{V} \Leftrightarrow V = 0{,}00149\ L = 1{,}49\ mL$ of DMSO

3. ACUTE BRAIN SLICE ELECTROPHYSIOLOGY

For each day of experiments, one animal was used, giving rise to 8-10 available brain slices per animal.

3.1. Mouse anesthesia and euthanasia

In order to be anesthetized, P20 to P26 mice were placed for 2 minutes in a transparent acrylic chamber that was rapidly filled with compressed gas containing 5% of isoflurane. Absence of reflex upon paw or tail pinching was always checked prior to decapitation.

3.2. Acute brain slices preparation

After decapitation, the animal's head was placed in a petri dish filled with ice-cold cutting solution composed of (in mM) 200 sucrose, 25 $NaHCO_3$, 20 glucose, 2,5 KCl, 1,25 NaH_2PO_4, 0,5 $CaCl_2$ and 7 $MgCl_2$. This solution was continuously oxygenated with carbogen (95% O_2/ 5% CO_2). The skull and subsequently the whole brain containing the two hippocampi were removed from the animal's head, making sure that the brain was submerged all the time.

Parasagittal slices with 300 µm of thickness were obtained on a Leica VT1200S vibratome (Leica Microsystems GmbH) in a continuously oxygenated ice-cold cutting solution. After slicing, they were kept in artificial cerebrospinal fluid (ACSF) at 35°C for approximately 30 minutes. This ACSF was composed of (in mM) 120 NaCl, 16,5 glucose, 1 $MgCl_2$ (anydrous), 2 $CaCl_2$ (2 $\cdot H_2O$), 2,5 KCl, 1,25 NaH_2PO_4 (H_2O), 26 $NaHCO_3$, 0,5 ascorbate (305 mOsm/L), always being oxygenated with carbogen. After 30 minutes, slices were left at room temperature (RT).

3.3. Slice electrophysiology

Slices were kept in RT oxygenated ACSF for no longer than 6 hours. In the recording chamber, they were continuously perfused with the previously described ACSF and supplemented with bicuculline (10 µM) and D-AP5 (50 µM), in order to block $GABA_A$ receptors and NMDA receptors, respectively. The circuit was kept closed and the flow remained constant through the protocols done.

Different regions of the hippocampus (namely DG, hilus, CA3 and CA1 pyramidal cells) were identified under infrared illumination with differential interference contrast optics (Micro Manager 1.4). Micropipettes (3,5–6 MΩ) were prepared from borosilicate glass capillaries (World Precision Instruments®) using a P-97 puller (Sutter Instrument). Recording pipettes were filled with an intracellular solution composed of (in mM) 125 $CsCH_3SO_3$, 2 $MgCl_2$-$6H_2O$, 4 NaCl, 10 EGTA, 10 HEPES, 5 P-Creatine, 5 NaATP (pH 7,3 adjusted using CsOH; 300 mOsm/L). CA3 pyramidal cells were recorded in whole-cell voltage-clamp mode, at RT. This clamping was held at -70 mV using a HEKA EPC 9/10 amplifier under the control of

PatchMaster® software. Access resistance was regularly monitored during recordings, and cells were rejected if it changed > 10% during the experiment. Mf-EPSCs were elicited by poking deeply the hilus upper region with a patch pipette filled with extracellular solution (previously described ACSF) until synaptic responses with the characteristic features of MFs were found: 1) high variability of EPSCs amplitudes when stimulating at 1 Hz; 2) fast onset and slow decay EPSCs when stimulating at 1 Hz; 3) frequency facilitation when stimulating at 1 Hz and 3 Hz; 4) occurrence of failure(s) when stimulating at 0.1 Hz; 5) absence of EPSCs with the addition of LCCG-I. Hereafter, three different protocols were performed: Protocol 1, Protocol 2 and Protocol 3.

- **Protocol 1:**

Protocol 1 (Fig. 3) was performed for every experimental drug: UBP310, LCKE10, LC29, P03, BPAM344, ATM 2_21 and ATM 2_32. After the stimulating pipette and recording pipette were both placed, Protocol 1 started with a 30 sweeps stimulation at a frequency of 0.1 Hz. After this first stimulation, 60 sweeps at a frequency of 3 Hz were applied. Next, LY303070 (25 µM) was applied into the circuit and left acting for 5 minutes. After this time, a new 3 Hz stimulation of 60 sweeps was done, in order to isolate the KAR-EPSCs. Finally, to test the experimental drug, the latter was applied into the circuit (20 µM was the concentration used for each experimental drug, besides UBP310, which was 3 µM) and left acting for 5 minutes. Again, a new 3 Hz stimulation of 60 sweeps was applied.

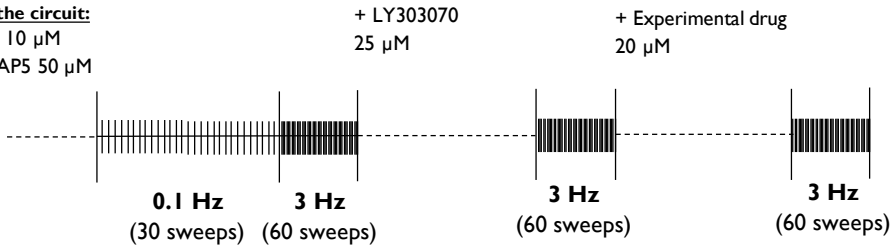

Figure 3 | Representative scheme of electrophysiology Protocol 1.

- **Protocol 2:**

Protocol 2 (Fig. 4) was performed only for the most interesting drug found in Protocol 1, this is, the drug that most effectively inhibited KAR-EPSCs. Thus, after adding bicuculline 10 µM, D-AP5 50 µM and LY303070 25 µM into the circuit in order to isolate KAR-EPSCs, increasing concentrations of the most interesting drug were progressively added to the bath, and each new concentration was left to act for 5 minutes, before applying a new stimulation of 3 Hz. Eight increasing concentrations were used in order to build a dose-response curve for this

pharmacological compound: t_1 (30 nM), t_2 (100 nM), t_3 (300 nM), t_4 (1 µM), t_5 (3 µM), t_6 (10 µM), t_7 (30 µM) and t_8 (100 µM).

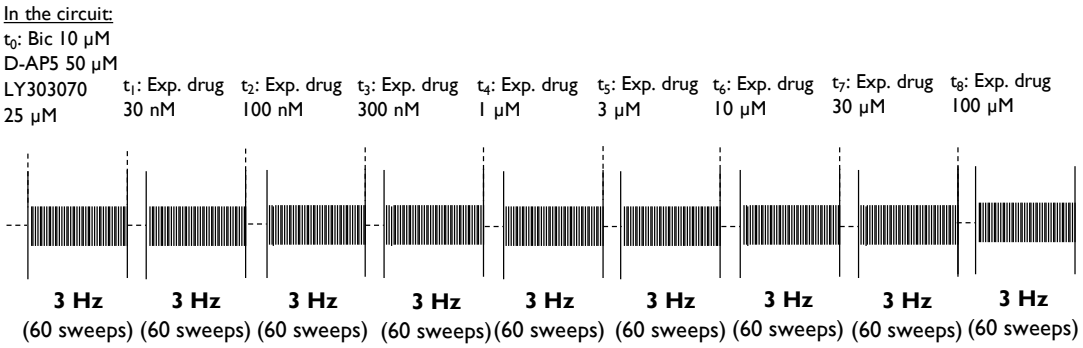

Figure 4 | Representative scheme of electrophysiology Protocol 2.

- **Protocol 3:**

As Protocol 2, Protocol 3 (Fig. 5) was performed only for the most interesting drug which was found in Protocol 1. Thus, Protocol 3 started with 30 sweeps of paired-pulse stimulation (PP40) with an interval of 40 ms between each pulse and with an interval of 40 s between each burst. At the end of the PP40 protocol, 60 sweeps with a frequency of 3 Hz were applied. The next step was to apply the experimental drug into the circuit and wait 5 minutes. After these 5 minutes, the same stimulations were applied, this is, PP40 and 3Hz.

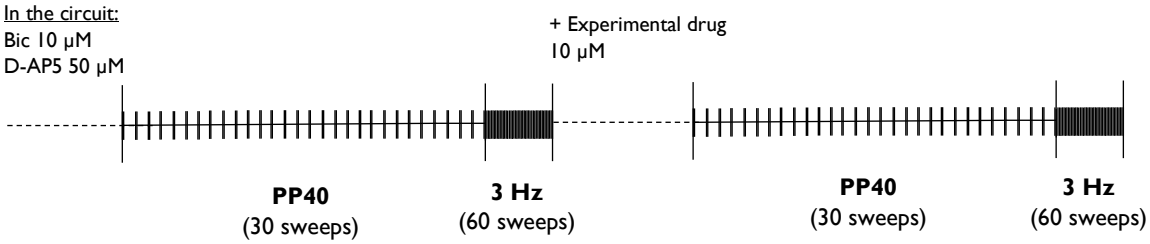

Figure 5 | Representative scheme of electrophysiology Protocol 3.

3.4. Data analysis

Data were analysed in Igor Pro 6. Cells were discarded from analysis if access resistance varied by 10% or more during recordings.

4. STATISTICAL ANALYSIS

Data plotting and statistical analyses were performed with GraphPad Prism 8.0 (GraphPad Software, La Jolla, CA, USA). Values were first tested for normality (Shapiro-Wilk and Kolmogorov-Smirnov tests). Data were presented as scatter plots with mean or median,

according to the result of the normality test. Normally distributed data were compared using paired t-test or an ordinary one-way ANOVA, while non-normally distributed data were compared using Wilcoxon test or Kruskal-Wallis test. Statistical significance was defined at a p-value lower than 0.05. *$p < 0.05$, **$p < 0.01$, ***$p < 0.001$.

III. RESULTS

1. PUTATIVE ORTHOSTERIC ANTAGONISTS OF GLUK2/GLUK5 KARS

The first set of experiments was performed for the group of putative orthosteric antagonists of GluK2/GluK5 KARs. This group included LCKE10, LC29 and P03. All the recordings performed for these compounds took into consideration UBP310 as a reference molecule. UBP310 is known to inhibit GluK1 and GluK3 homomeric KARs as well as postsynaptic KARs at mf-CA3 synapses, which are likely composed of heteromeric GluK2/GluK5 KARs. UBP310 spares GluK2/GluK3 KARs at the presynaptic terminal, which are important players for synaptic plasticity at this synapse, as well as AMPARs (Perrais *et al*., 2009; Pinheiro *et al*., 2013). Thus, the first compound to be tested was UBP310, being considered as a positive control for the following experiments. In this way, in these experimental conditions, all the pharmacological compounds giving rise to results comparable with UBP310 were considered potential new selective orthosteric antagonists of GluK2/GluK5 KARs.

1.1. For every experimental group of CA3 PCs, each one showed comparable basal synaptic transmission, frequency facilitation and AMPAR/KARs distribution upon MF stimulation

Starting with Protocol 1 (see Materials and Methods), several analyses were performed for each group of CA3 PCs, concerning the moment prior to compound application in the circuit (UBP310 PCs group, n=11; LCKE10 PCs group, n=13; LC29 PCs group, n=11; and P03 PCs group, n=10), namely: 1) AMPAR+KAR EPSCs peak amplitudes at 0.1 Hz, to indirectly measure synaptic transmission at a low frequency of stimulation (Fig. 1A); 2) the ratio between AMPAR+KAR EPSCs peak amplitudes at 3 Hz and 0.1 Hz, to measure the extent of frequency facilitation at mf-CA3 synapses (Fig. 1B); 3) the percentage of KAR-EPSCs peak amplitudes over AMPA+KAR EPSCs peak amplitudes (Fig. 1C); and, 4) to have a clearer view of the AMPAR/KARs distribution at mf-CA3 synapses, a graphical representation of AMPAR+KAR EPSCs peak amplitudes as a function of KAR-EPSCs peak amplitudes (Fig. 1D). Representative traces of pharmacologically isolated AMPAR+KAR EPSCs at 0.1 Hz and 3 Hz prior to compound application show a strong frequency facilitation at mf-CA3 synapses for each experimental group of CA3 PCs (Supplementary data - Figure 1). All these first analyses revealed comparable features of mf-CA3 synapses for each experimental group of CA3 PCs in terms of basal synaptic transmission, frequency facilitation and AMPAR/KARs distribution. The statistical significance found in Fig. 1C between LC29 and P03 groups was not considered biologically relevant at mf-CA3 synapses.

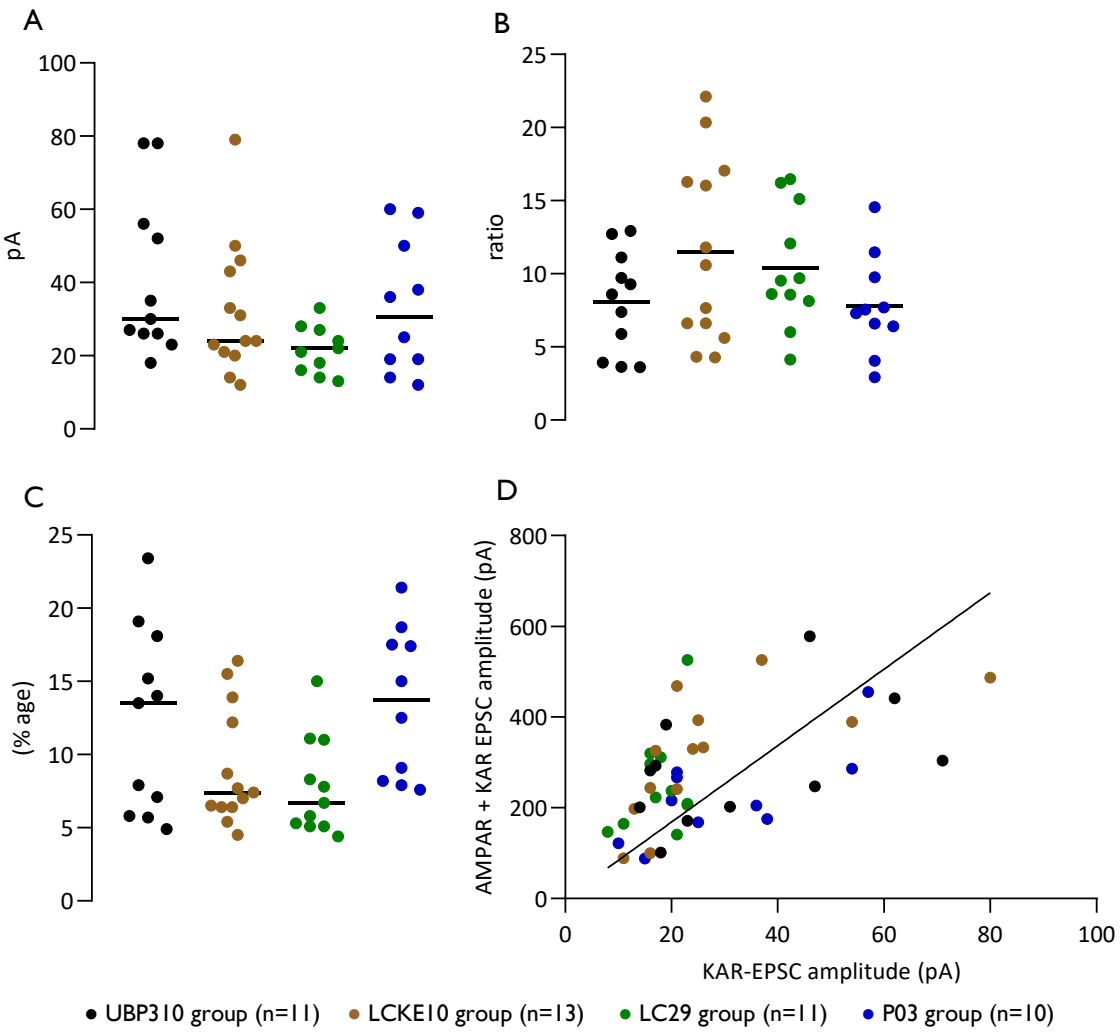

Figure 1 | Mossy fiber (MF) stimulation at 0.1 Hz and 3 Hz shows similar properties regarding basal synaptic transmission, frequency facilitation and AMPAR/KARs distribution at CA3 PCs, for all experimental groups of CA3 PCs, prior to compound application. **A** Scatter plot indicating the amplitude (pA) of AMPA+KAR EPSCs upon 0.1 Hz stimulation for each group (median is represented as a black bar in each column; Kruskal-Wallis test, P>0.05 (ns) in multiple comparisons); **B** Scatter plot of different frequency facilitation ratios for each group of CA3 PCs (mean represented as a black bar in each column; ordinary one-way ANOVA test, P>0.05 (ns) in multiple comparisons); **C** Scatter plot indicating the percentage (%) of KAR-EPSCs over AMPA+KAR EPSCs in mf-CA3 synapse for each group of CA3 PCs (median is represented as a black bar in each column; Kruskal-Wallis test, P>0.05 (ns) in multiple comparisons, except for LC29 group vs. P03 group, in which P<0.05 (*)); **D** Scatter plot representing the AMPAR+KAR EPSCs peak amplitudes as a function of KAR-EPSCs peak amplitudes distribution at mf-CA3 synapses.

1.2. UBP310 decreases peak amplitude, synaptic charge and decay time of KAR-EPSCs at mf-CA3 synapses

Proceeding with Protocol 1, the effects of UBP310 were tested on pharmacologically isolated KAR-EPSCs at mf-CA3 synapses. As described in Materials and Methods section, KAR-EPSCs were pharmacologically isolated by applying bicuculine (10 μM), D-AP5 (50 μM) and LY303070 (25 μM) in the circuit, in order to block $GABA_AR$, NMDAR and AMPAR, respectively (Fig. 2A). After having KAR-EPSCs isolated, UBP310 (3 μM) was applied in the circuit for 5 min.

UBP310 effectively inhibited KAR-EPSCs peak amplitudes (Fig. 2B (representative unscaled traces), leading to an average remaining KAR-EPSCs peak amplitude of 37 ± 3% (Fig. 1D). Additionally, it could be observed that KAR-EPSCs decayed faster, meaning that the slow currents were preferentially inhibited, remaining the fast currents (Fig. 2C (representative scaled traces)). This also explained smaller remaining KAR-EPSCs synaptic charge (Fig. 2E) (19 ± 2%) after compound application, as compared with peak amplitude. The decay times (τ) were also measured, before and after compound application, and they decreased from 37 ± 5 ms to 10 ± 2 ms. This decrease was statistically significant (Fig. 2F).

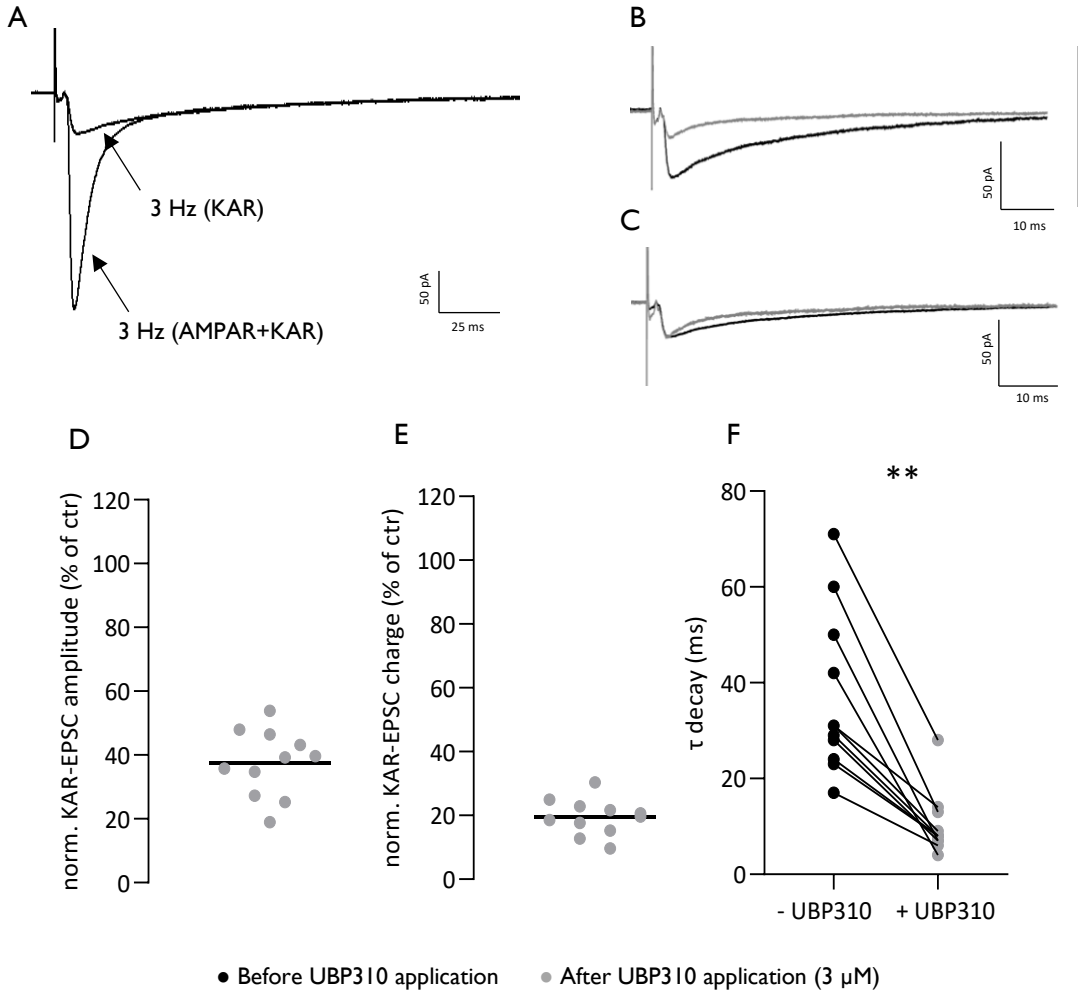

Figure 2 | UBP310 decreases peak amplitude, synaptic charge and decay time of KAR-EPSCs at mf-CA3 synapses. **A** Representative traces of pharmacologically isolated AMPA+KAR EPSCs and KAR-EPSCs, both at 3 Hz (average of 50 traces) at mf-CA3 synapses, prior to UBP310 application; **B** Representative KAR-EPSCs average traces at 3 Hz before (black trace) and after (grey trace) applying UBP310 (3 μM; average of 50 traces; not scaled); **C** Representative KAR-EPSCs average traces at 3 Hz before (black trace) and after (grey trace) applying UBP310 (3 μM; average of 50 traces; scaled); scale bars represented at bottom right; **D** Scatter plot with percentages of remaining KAR-EPSCs peak amplitudes after UBP310 application (3 μM; n=11; mean represented as a black bar (37 ± 3%;)); **E** Scatter plot with percentages of remaining KAR-EPSCs synaptic charge after UBP310 application (3 μM; n=11; mean represented as a black bar (19 ± 2%)); **F** Scatter plot indicating the different KAR-EPSCs decay times (τ) before (black) and after (grey) UBP310 application (3 μM) in the circuit (Wilcoxon test, n=11, P<0.01 (**)).

1.3. P03 is the most effective KAR antagonist

We next tested LCKE10, LC29 or P03 (20 μM) on pharmacologically isolated KAR-EPSCs. Comparing KAR-EPSCs at 3 Hz, before and after each compound application (LCKE10 - Fig. 3A, LC29 - Fig. 4A and P03 - Fig. 5A, for representative unscaled traces), it was observed that the three compounds decreased KAR-EPSCs peak amplitudes, leading to an average of remaining KAR-EPSCs peak amplitudes of 72 ± 3% for LCKE10 (n=13) (Fig. 3C), 50 ± 5% for LC29 (n=11) (Fig. 4C) and 34 ± 3% for P03 (n=10) (Fig. 5C). Similarly, these three compounds reduced KAR-EPSCs synaptic charge, leading to an average of remaining KAR-EPSCs synaptic charge of 82 ± 5% for LCKE10 (n=13) (Fig. 3D), 38 ± 4% for LC29 (Fig. 4D) and 14 ± 2% for P03 (Fig. 5D).

The scaled traces for LCKE10 (Fig. 3B) indicate that KAR-EPSCs decayed slightly slower in the presence of the compound. The comparison of decay times prior and after LCKE10 application shows a statistically significant increase between these values (Fig. 3E). In contrast, KAR-EPSCs decayed faster in presence of LC29 or P03, remaining mostly the fast currents (Fig. 4B and 5B, respectively). The decrease in the decay times for both compounds (Fig. 4E and 5E) was statistically significant.

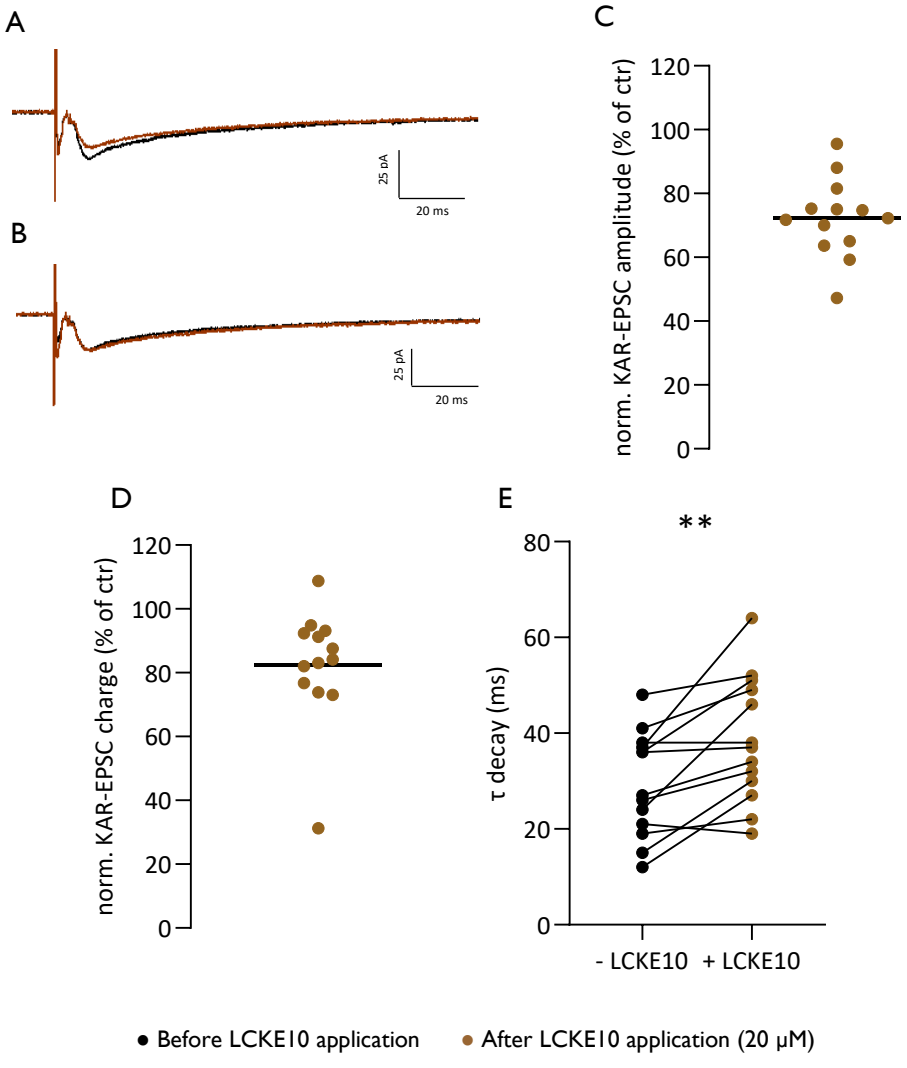

Figure 3 | LCKE10 moderately decreases KAR-EPSCs peak amplitude and synaptic charge but increases its decay time at mf-CA3 synapses. **A** Representative KAR-EPSCs average traces at 3 Hz before (black trace) and after (brown) LCKE10 application (20 μM; average of 50 traces; not scaled); **B** Representative KAR-EPSCs average traces at 3 Hz before (black trace) and after (brown) applying LCKE10 (20 μM; average of 50 traces; scaled); scale bars represented at bottom right; **C** Scatter plot with percentages of remaining KAR-EPSCs peak amplitude after LCKE10 application (20 μM; mean is represented as a black bar (72 ± 3%)); **D** Scatter plot with percentages of reduction of KAR-EPSCs synaptic charge by LCKE (20 μM; mean is represented as a black bar (82 ± 5%)); **E** Scatter plot indicating KAR-EPSCs decay time (τ) before (black) and after (brown) LCKE10 application (20 μM) in the circuit (paired t-test, n=13, P <0.01 (**)).

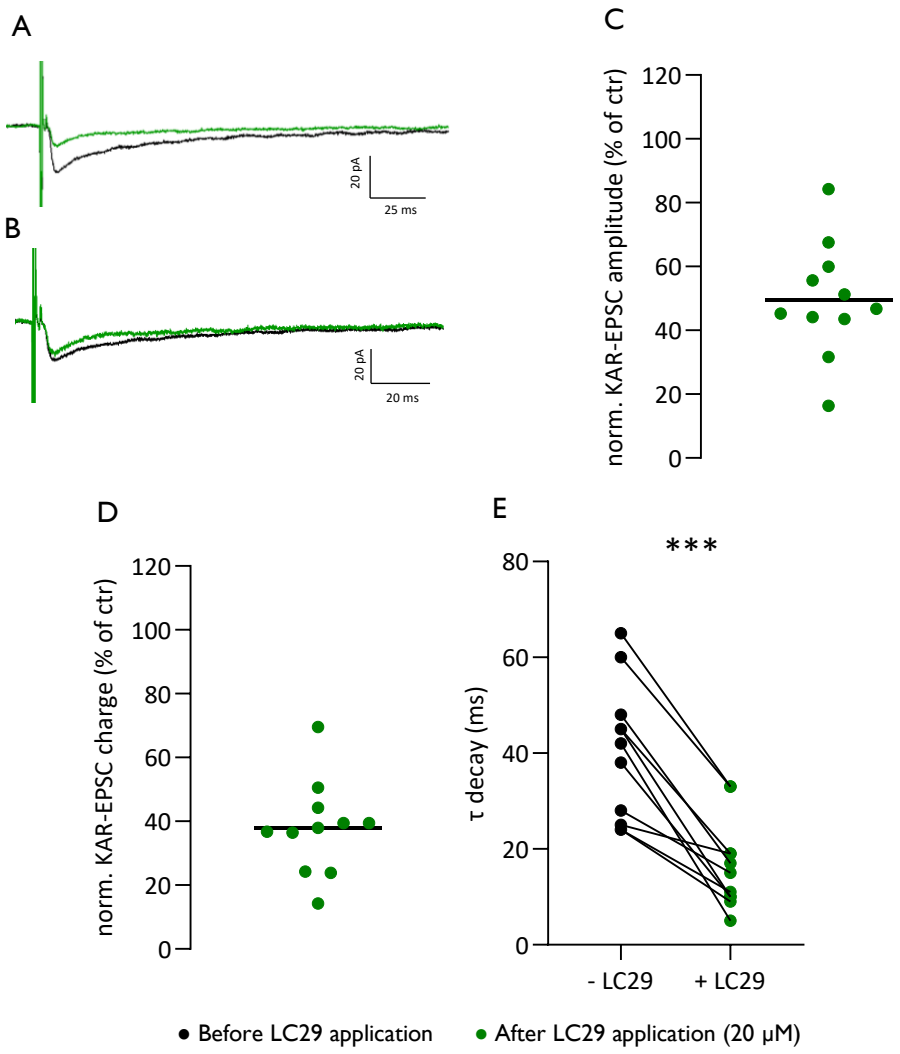

Figure 4 | LC29 decreases KAR-EPSCs peak amplitude, synaptic charge and decay time at mf-CA3 synapses. **A** Representative KAR-EPSCs average traces at 3 Hz before (black trace) and after (green) LC29 application (20 μM; average of 50 traces; not scaled); **B** Representative KAR-EPSCs average traces at 3 Hz before (black trace) and after (green) applying LC29 (20 μM; average of 50 traces; scaled); scale bars represented at bottom right; **C** Scatter plot with percentages of remaining KAR-EPSCs peak amplitude after LCKE application (20 μM; mean is represented as a black bar (50 ± 5%)); **D** Scatter plot with percentages of remaining KAR-EPSCs synaptic charge after LCKE application (20 μM; mean is represented as a black bar (38 ± 4%)); **E** Scatter plot indicating KAR-EPSCs decay time (τ) before (black) and after (green) LC29 application (20 μM) in the circuit (paired t-test, n=11, P <0.001 (***)).

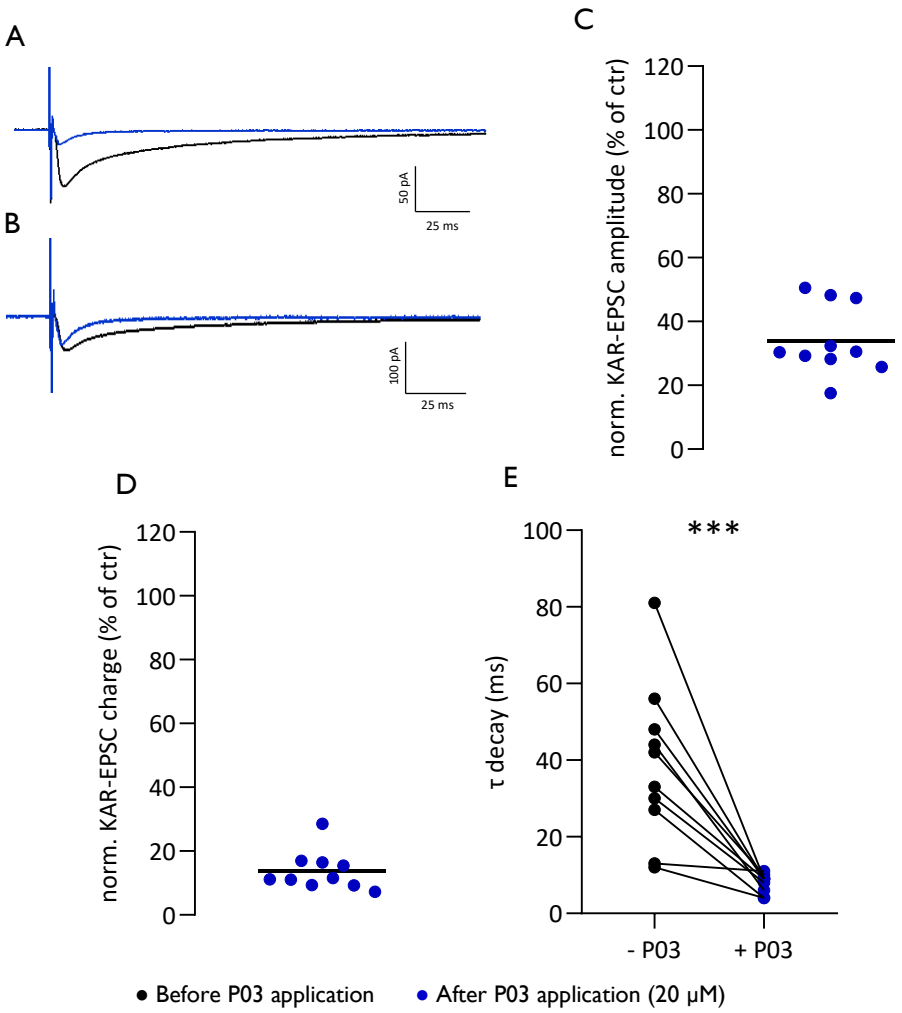

Figure 5 | P03 largely decreases KAR-EPSCs peak amplitude, synaptic charge and decay time at mf-CA3 synapses. **A** Representative KAR-EPSCs average traces at 3 Hz before (black trace) and after (blue) P03 application (20 μM; average of 50 traces; not scaled); **B** Representative KAR-EPSCs average traces at 3 Hz before (black trace) and after (blue) applying P03 (20 μM; average of 50 traces; scaled); scale bars represented at bottom right; **C** Scatter plot with percentages of remaining KAR-EPSCs peak amplitude after P03 application (20 μM; mean is represented as a black bar (34 ± 3%)); **D** Scatter plots with percentages of remaining KAR-EPSCs synaptic charge after P03 application (20 μM; mean is represented as black bar (14 ± 2%)); **E** Scatter plot indicating KAR-EPSCs decay times (τ) before (black) and after (blue) P03 application (20 μM) in the circuit (paired t-test, n=10, P <0.001 (***)).

The inhibition of the peak amplitude and synaptic charge of KAR-EPSCs for each compound was represented and compared with the positive control UBP310. The data was plotted considering the remaining KAR-EPSCs peak amplitudes or synaptic charges. Among these experimental compounds, P03 was the most potent, inhibiting KAR-EPSCs peak amplitudes (34 ± 3%) (Fig. 6A), reducing synaptic charges (14 ± 2%) (Fig. 6B) and showing a higher reduction in decay times (-73 ± 7%) (Fig. 6C).

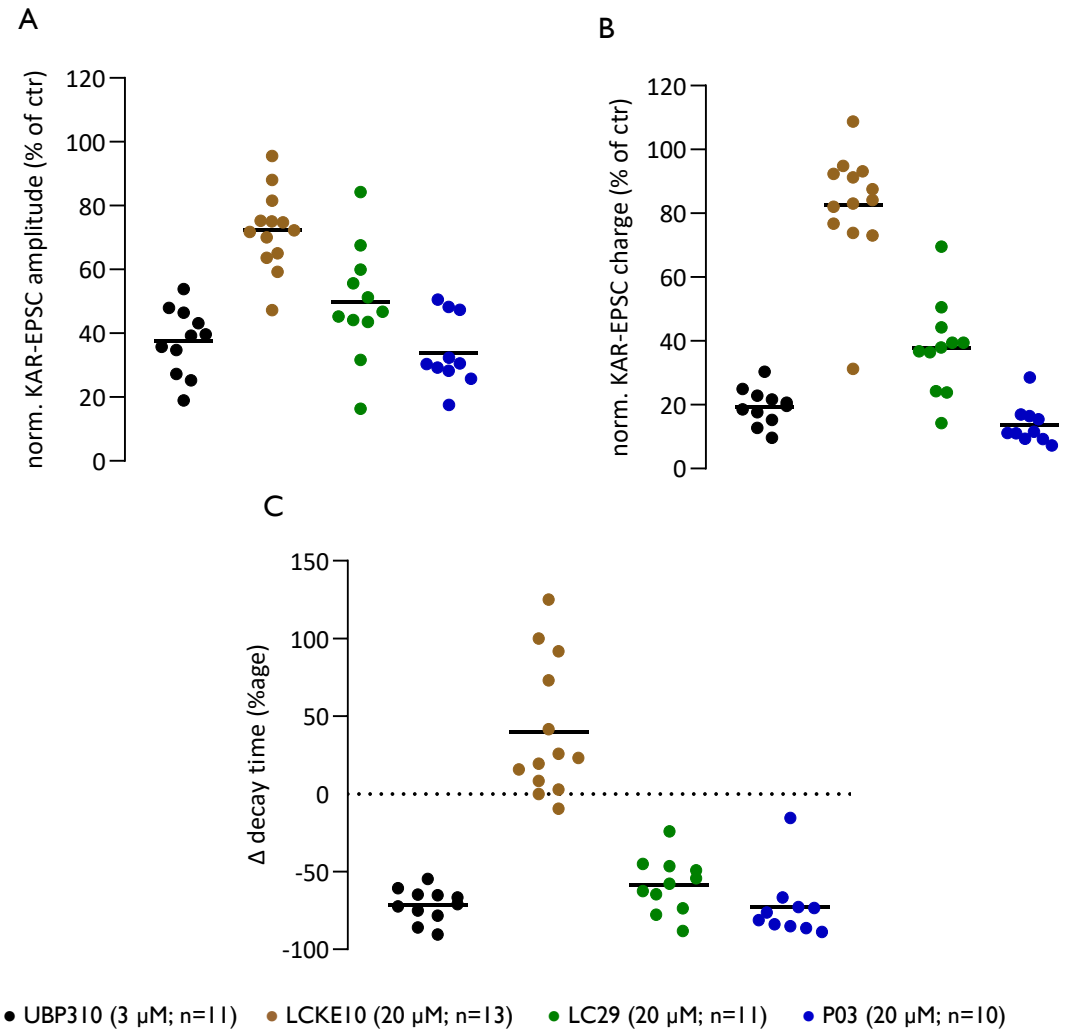

Figure 6 | P03 is the most effective pharmacological compound decreasing KAR-EPSCs peak amplitude, reducing their synaptic charge and decreasing their decay time at mf-CA3 synapses. **A** Scatter plot showing the percentage of remaining KAR-EPSCs peak amplitude after UBP310 (black, 3 μM, n=11), LCKE10 (brown, 20 μM, n=13), LC29 (green, 20 μM, n=11) and P03 (blue, 20 μM, n=10); mean values are represented as a black bar for each compound (UBP310: 37 ± 3%; LCKE10: 72 ± 3%; LC29: 50 ± 5%; P03: 34 ± 3%); **B** Scatter plot showing the percentage of remaining KAR-EPSCs synaptic charge after UBP310 (black, 3 μM, n=11), LCKE10 (brown, 20 μM, n=13), LC29 (green, 20 μM, n=11) or P03 (blue, 20 μM, n=10) application; mean values are represented as a black bar for each compound (UBP310: 19 ± 2%; LCKE10: 82 ± 5%; LC29: 38 ± 4%; P03: 14 ± 2%); **C** Scatter plot showing the variation in decay times by UBP310 (black, 3 μM, n=11), LCKE10 (brown, 20 μM, n=13), LC29 (green, 20 μM, n=11) and P03 (blue, 20 μM, n=10); mean values are represented as a black bar for each compound (UBP310: -71 ± 3%; LCKE10: 40 ± 12%; LC29: -58 ± 5%; P03: -73 ± 7%).

2. PUTATIVE ALLOSTERIC MODULATORS OF GLUK2/GLUK5 KARS

A second set of experiments was performed to test the effects of putative allosteric modulators of GluK2/GluK5 KARs. The compounds tested were BPAM344, ATM 2_21 and ATM 2_32. BPAM344 has been previously described as a positive allosteric modulator of recombinant GluK2a, GluK3a, GluK1b and $GluA1_i$ (Larsen *et al*., 2017). In this set of experiments, BPAM344 was used as a control, however, the limited number of cells tested (n=3) was due to the fact that in this specific project the main goal was to validate and characterize mainly negative allosteric modulators of GluK2/GluK5 KARs, as will be further discussed.

2.1. Comparable synaptic parameters for all experimental groups at mf-CA3 PCs synapses

The analysis of several synaptic parameters was performed for each group of CA3 PCs prior to the application of any putative allosteric modulator (BPAM344 PCs group, n=3; ATM 2_21 PCs group, n=12; ATM 2_32 PCs group, n=10), namely: 1) AMPAR + KAR-EPSCs peak amplitudes at 0.1 Hz, to indirectly measure basal synaptic transmission (Fig. 7A); 2) the ratio between AMPAR+KAR EPSCs peak amplitudes at 3 Hz and 0.1 Hz, to measure the extent of frequency facilitation at mf-CA3 synapses (Fig. 7B); 3) the relative peak amplitude of KAR-EPSCs over AMPA+KAR EPSCs (Fig. 7C) and, 4) a graphical representation of AMPAR+KAR EPSCs peak amplitudes as a function of KAR-EPSCs peak amplitudes (Fig. 7D).

For each experimental group of CA3 PCs, representative traces of pharmacologically isolated AMPAR+KAR EPSCs at 0.1 Hz and 3 Hz stimulations show frequency facilitation at mf-CA3 synapses prior to compound application (Supplementary data - Figure 1). As described in section 1., all these first analyses revealed comparable features of mf-CA3 synapses in each experimental group of CA3 PCs in terms of basal synaptic transmission, frequency facilitation and AMPAR/KARs distribution.

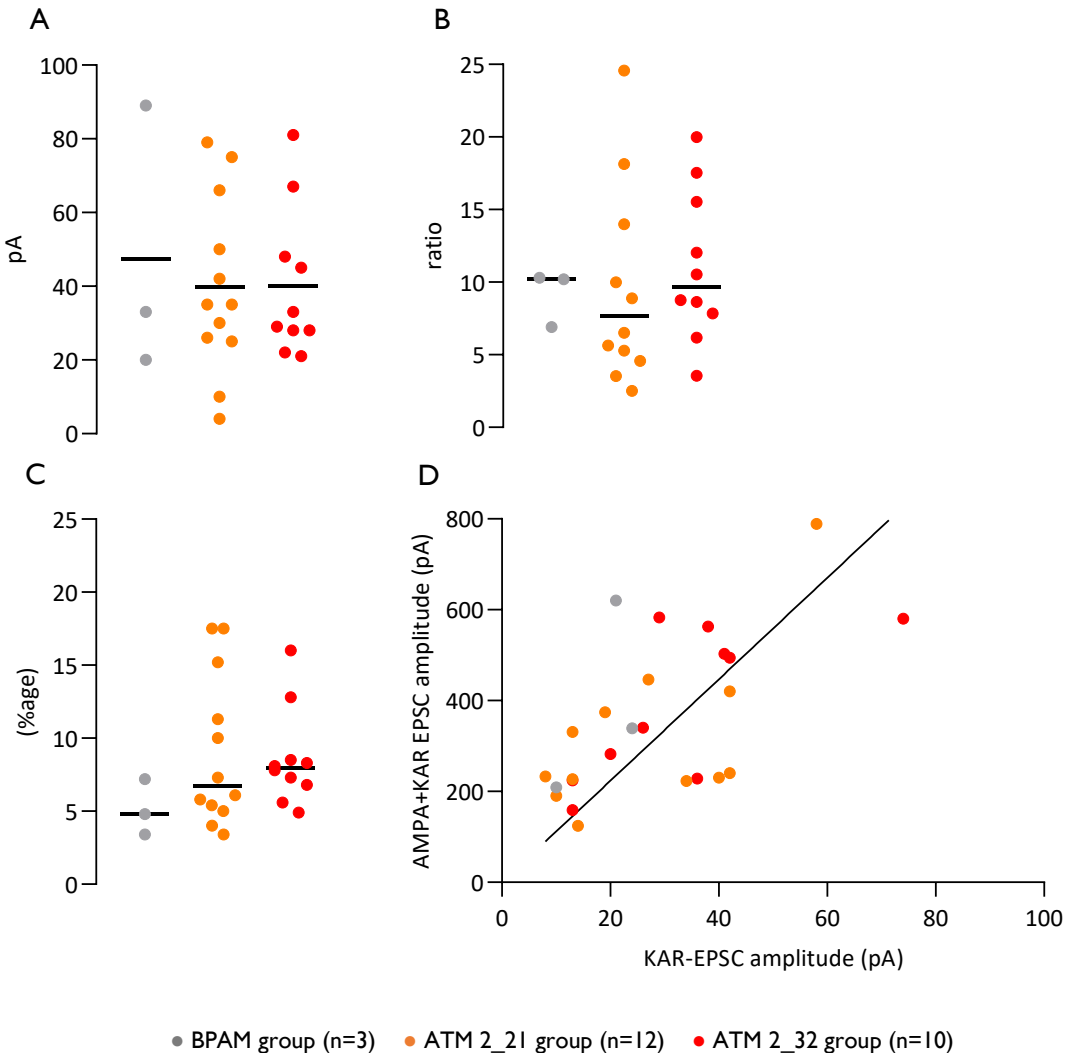

Figure 7 | Mossy fiber (MF) stimulation at 0.1 Hz and 3 Hz shows similar properties regarding basal synaptic transmission, frequency facilitation and AMPAR/KARs distribution at CA3 PCs, for all experimental groups of CA3 PCs, prior to compound application. **A** Scatter plot indicating the peak amplitude (pA) of AMPA+KAR EPSCs upon 0.1 Hz stimulation for each group (mean is represented as a black bar in each column; ordinary one-way ANOVA test, P>0.05 (ns) in multiple comparisons); **B** Scatter plot of different frequency facilitation ratios for each group (median represented as a black bar in each column; Kruskal-Wallis test, P>0.05 (ns) in multiple comparisons); **C** Scatter plot indicating the percentage (%) of KAR-EPSCs peak amplitudes over AMPA+KAR EPSCs peak amplitudes in mf-CA3 synapses for each group (median is represented as a black bar in each column; Kruskal-Wallis, P>0.05 (ns) in multiple comparisons); **D** Scatter plot representing the AMPAR+KAR EPSCs peak amplitudes as a function of KAR-EPSCs peak amplitudes distribution at mf-CA3 synapses.

2.2. BPAM344 potentiates KAR-EPSCs peak amplitudes at mf-CA3 synapses

In order to test the effect of BPAM344 on the peak amplitudes of KAR-EPSCs, the concentration used in the circuit was 20 µM. Comparing KAR-EPSCs at 3 Hz, before and after BPAM344 application, there was an increase of KAR-EPSCs peak amplitudes of 162 ± 34 % (n=3) after 5 minutes and of 168 ± 24% (n=3) after 10 minutes (Fig. 8A and 8C). Regarding the slow

and fast KAR currents both seemed to be equally potentiated (Fig. 8B), with no statistically significant differences in decay times before and after compound application (Fig. 8D).

These experiments show that BPAM344 likely act on native KARs, potentiating KAR-EPSCs peak amplitude at mf-CA3 synapses. However, the effect could either be due to presynaptic and/or postsynaptic KARs. Additionally, BPAM344 may also be acting on AMPA receptors (not tested). Further analyses would be required, namely: 1) a higher number of recorded cells; 2) a second Protocol to confirm its selectivity to postsynaptic GluK2/GluK5 KARs (e.g. Protocol 3 – see Materials and Methods).

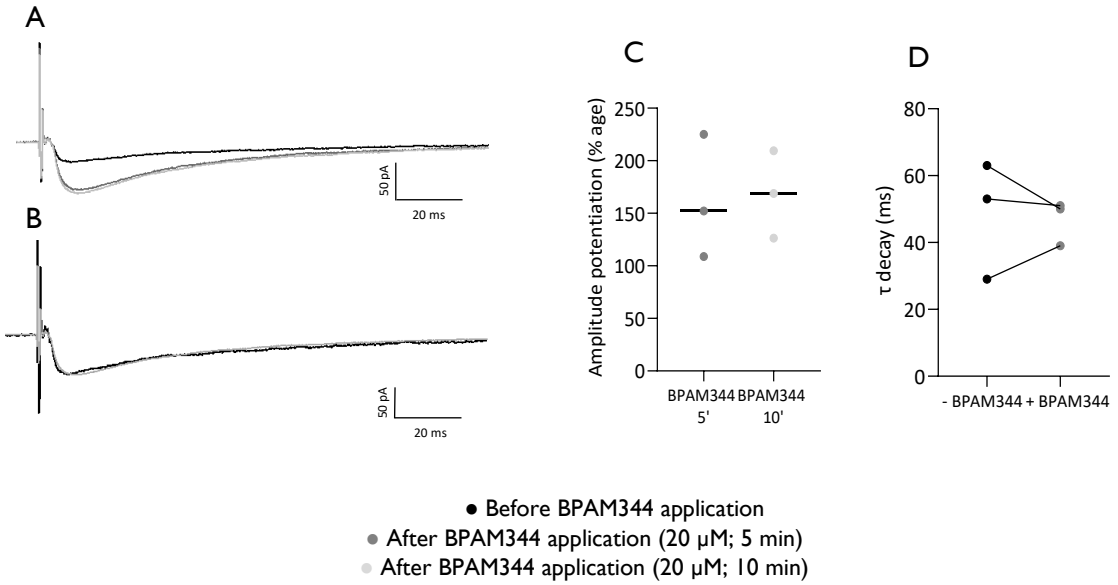

Figure 8 | BPAM344 potentiates KAR-EPSCs peak amplitudes at mf-CA3 synapses. **A** Representative KAR-EPSCs average traces at 3 Hz before (black) and after 5 minutes (dark grey) or 10 minutes (light grey) of BPAM344 application (20 μM; average of 50 traces; not scaled); **B** Representative KAR-EPSCs average traces at 3 Hz before (black) and after 10 minutes (light grey) of BPAM344 application (20 μM; average of 50 traces; scaled); scale bars represented at bottom right; **C** Scatter plot with percentages of KAR-EPSCs peak amplitudes potentiation by BPAM344 (20 μM; medians are represented as black bars; Wilcoxon test, P>0.05 (ns)); **D** Scatter plot indicating KAR-EPSCs decay times before (black) and after BPAM344 application (5 minutes) (dark grey) (Wilcoxon test, P>0.05 (ns)).

2.3. Putative positive allosteric modulators ATM 2_21 and ATM 2_32 partially decrease KAR-EPSCs peak amplitude and synaptic charge, increasing their decay time at mf-CA3 synapses

We tested the effect of ATM 2_21 and ATM 2_32 on KAR-EPSCs recorded at 3 Hz. Both compounds decreased the peak amplitude of KAR-EPSCs to a small extent, specifically to 75 ± 4% for ATM 2_21 (n=12) (Fig. 9A (unscaled traces) and 9C) and 83 ± 6% for ATM 2_32 (n=10) (Fig. 10A (unscaled traces) and 10C). ATM 2_21 reduced the synaptic charge of KAR-EPSCs moderately (reduction to 82 ± 6%) (Fig. 9D), whereas ATM 2_32 did not impact the charge of KAR-EPSCs (103 ± 7%) (Fig. 10D). The scaled traces for both compounds indicate that KAR-EPSCs decayed slower after compound application (Fig. 9B and 10B). This was also confirmed

by the comparison of KAR-EPSCs decay times before and after compound application, in which there was a statistically significant increase in the decay times for both compounds (Fig. 9E and 10E).

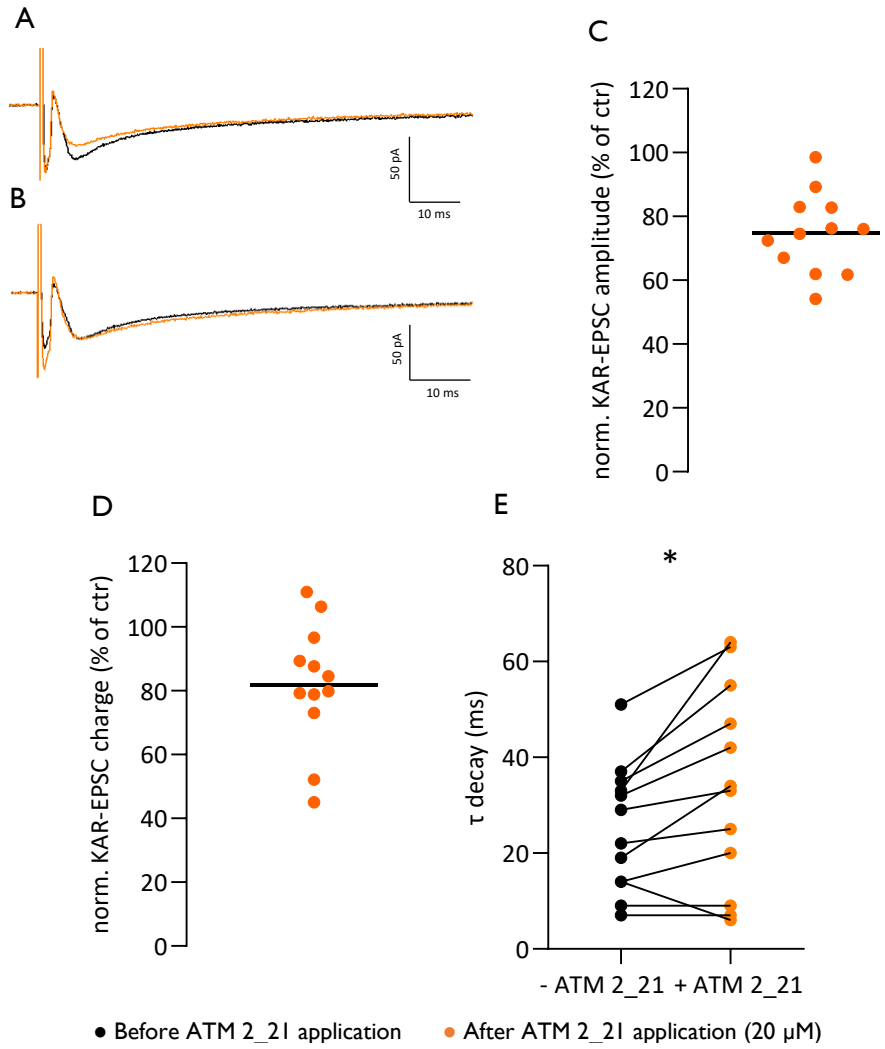

Figure 9 | ATM 2_21 partially decreases KAR-EPSCs peak amplitude and synaptic charge but increases their decay time. **A** Representative KAR-EPSCs average traces at 3 Hz before (black) and after (orange) of ATM 2_21 application (20 μM; average of 50 traces; not scaled traces); **B** Representative KAR-EPSCs average traces at 3 Hz before (black) and after (orange) ATM 2_21 application (20 μM; average of 50 traces; scaled traces); scale bars represented at bottom right; **C** Scatter plot with percentages of remaining KAR-EPSCs peak amplitudes after ATM 2_21 application (20 μM; mean is represented as a black bar (75 ± 4%); **D** Scatter plot with percentages of of remaining KAR-EPSCs synaptic charge after ATM 2_21 application (20 μM) (mean is represented as a black bar (82 ± 6%)); **E** Scatter plot indicating KAR-EPSCs decay time before (black) and after (orange) ATM 2_21 application (paired t test, n=12, P<0.05 (*)).

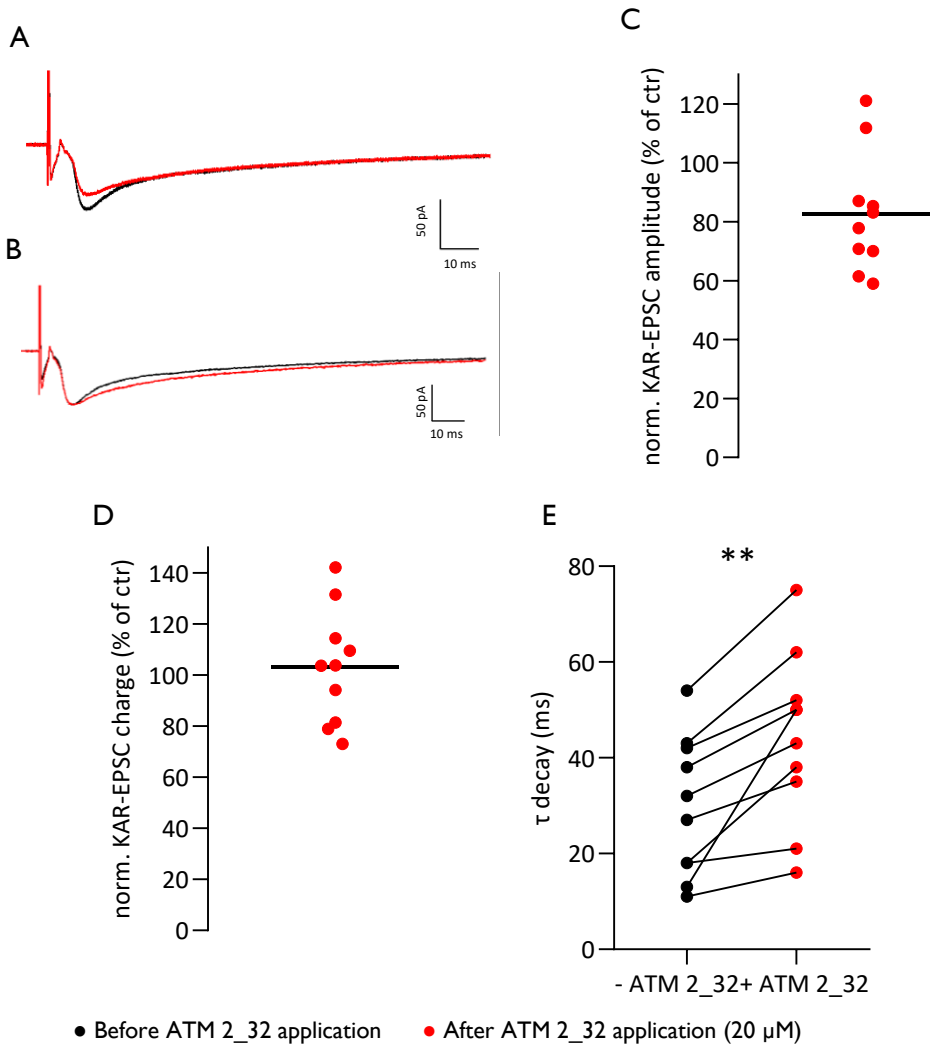

Figure 10 | ATM 2_32 partially decreases KAR-EPSCs peak amplitude, increasing their decay time, and not having a significant impact on their synaptic charge. **A** Representative KAR-EPSCs average traces at 3 Hz before (black) and after (red) of ATM 2_32 application (20 μM; average of 50 traces; not scaled traces); **B** Representative KAR-EPSCs average traces at 3 Hz before (black) and after (red) ATM 2_32 application (20 μM; average of 50 traces; scaled traces); scale bars represented at bottom right; **C** Scatter plot with percentages of remaining KAR-EPSCs peak amplitude after ATM 2_32 application (20 μM; mean is represented as a black bar (83 ± 6%)); **D** Scatter plot with percentages of remaining KAR-EPSCs synaptic charge after ATM 2_32 application (20 μM; mean is represented as a black bar (103 ± 7%)); **E** Scatter plot indicating KAR-EPSCs decay time before (black) and after (red) ATM 2_32 application (paired t test, n=12, P<0.01 (**)).

Additional analyses with a different electrophysiology protocol showed that ATM 2_21 increases AMPA+KAR EPSCs baseline (for 0.1 Hz and 3 Hz stimulations), decreases frequency facilitation and decreases paired-pulse ratio (n=3, 20 μM) (Supplementary data – Figure 2). These results suggested two main hypotheses: either that ATM 2_21 might be a positive allosteric modulator (PAM) of presynaptic KARs (GluK2/GluK3) and a negative allosteric modulator (NAM) of postsynaptic KARs (GluK2/GluK5) or it might be a PAM of AMPARs and a NAM of KARs (both pre- and postsynaptic). Further analyses are required.

3. COMPARATIVE ANALYSES OF PUTATIVE ORTHOSTERIC ANTAGONISTS AND PUTATIVE ALLOSTERIC MODULATORS OF GLUK2/GLUK5 KARS

3.1. Comparison of the effects of the different groups of compounds on KAR-EPSCs

In sum, among the group of compounds which were designed to be putative orthosteric antagonists, P03 was the most potent compound inhibiting KAR-EPSCs peak amplitude and reducing their synaptic charge at mf-CA3 synapses. Among the group of compounds which were designed to be allosteric modulators, ATM 2_21 and ATM 2_32 moderately decreased KAR-EPSCs peak amplitude, however, not impacting significantly their synaptic charge. In Figure 11, the extent of inhibition of compounds in these two different groups are compared. This indicates clearly that putative orthosteric antagonists inhibited peak amplitude and synaptic charge of KAR-EPSCs more effectively than putative allosteric antagonists.

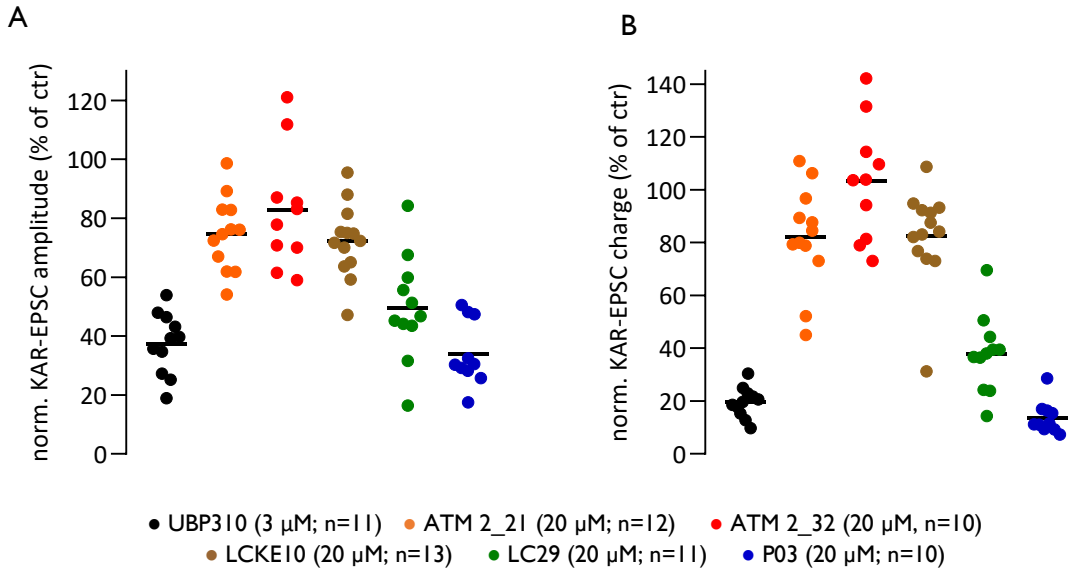

Figure 11 | Comparison of KAR-EPSCs reduction between different groups of compounds: UBP310 (black, 3 µM, n=11), ATM 2_21 (orange, 20 µM, n=12), ATM 2_32 (red, 20 µM, n=10), LCKE10 (brown, 20 µM, n=13), LC29 (green, 20 µM, n=11) and P03 (blue, 20 µM, n=10). **A** Scatter plot showing the percentage of remaining KAR-EPSCs peak amplitude after compound application; mean values are represented as a black bar for each compound (UBP310: 37 ± 3%; ATM 2_21: 75 ± 4% ; ATM 2_32: 83 ± 6%; LCKE10: 72 ± 3%; LC29: 50 ± 5%; P03: 34 ± 3%); **B** Scatter plot showing the percentage of remaining KAR-EPSCs synaptic charge after compound application; mean values are represented as a black bar for each compound (UBP310: 19 ± 2 %; ATM 2_21: 82 ± 6%; ATM 2_32: 103 ± 7%; LCKE10: 82 ± 5%; LC29: 38 ± 4 %; P03: 14 ± 2%).

3.2. Comparison of decay times and its variation between different groups of compounds

Comparing the initial and final decay times for all experimental groups (before and after compound application), it is possible to distinguish two different groups of compounds: a group in which the experimental compounds increase (moderately) the decay time of KAR-EPSCs (LCKE10, ATM 2_21 and ATM 2_32) and a group of experimental compounds which markedly decrease the decay time of KAR-EPSCs (UBP310, LC29 and P03) (Fig. 12A). Observing the variation of decay times for every experimental compound (Fig. 12B), it is even more evident these two different groups of compounds described.

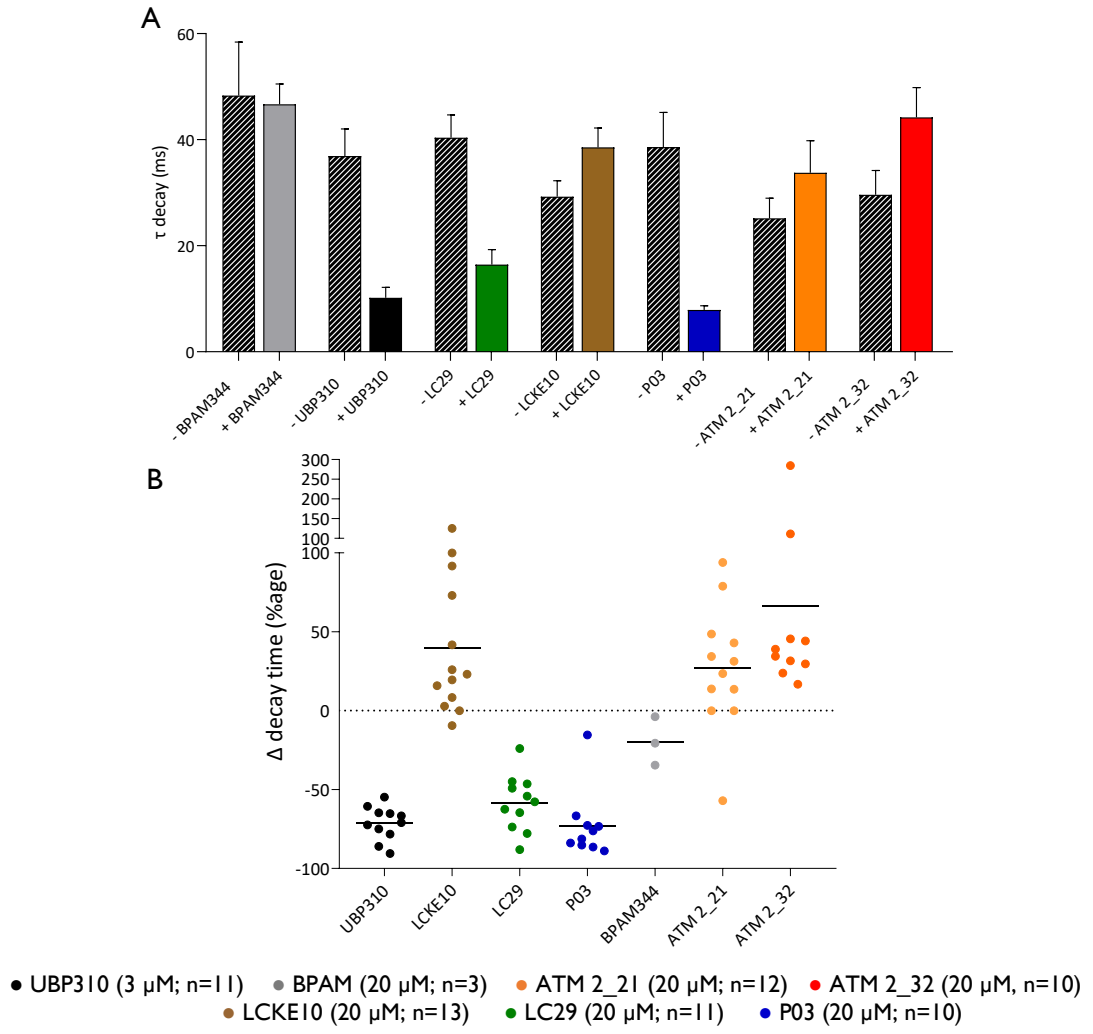

Figure 12 | Comparison between different groups of compounds regarding decay times (ms) and variation of decay times (%age): BPAM344 (grey, 20 μM, n=3), UBP310 (black, 3 μM, n=11), ATM 2_21 (orange, 20 μM, n=12), ATM 2_32 (red, 20 μM, n=10), LCKE10 (brown, 20 μM, n=13), LC29 (green, 20 μM, n=11) and P03 (blue, 20 μM, n=10); **A** Comparison between different groups of compounds regarding KAR-EPSCs decay time (ms) before and after compounds application; means and SEMs are represented (BPAM344: 47 ± 4 ms; UBP310: 10 ± 2 ms; LC29: 16 ± 3 ms; LCKE10: 39 ± 4 ms; P03: 8 ± 1 ms; ATM 2_21: 34 ± 6 ms; ATM 2_32: 44 ± 6 ms); **B** Scatter plot showing the variation in decay time by different groups of compounds (%age); means values are represented as a black bar for each compound (UBP310: -71 ± 3%; LCKE10: 40 ± 12%; LC29: -58 ± 5%; P03: -73 ± 7%; BPAM344: -20 ± 9%; ATM 2_21: 27 ± 11%; ATM 2_32: 66 ± 26%).

4. EXPLORING THE SELECTIVITY OF P03 FOR GLUK2/GLUK5 KARS

4.1. Dose-response curve analysis

We found that P03 was the most potent pharmacological compound decreasing both KAR-EPSC peak amplitudes and synaptic charge. Thus, the next set of experiments established a dose-response curve for P03 (Fig. 13). These experiments relied on applying the electrophysiology Protocol 2 (see Materials and Methods), where the KAR-EPSCs were first isolated and an increasing concentration of P03 was applied to the bath (30 nM → 100 nM → 300 nM → 1 µM → 3 µM →10 µM → 30 µM → 100 µM). Each concentration of P03 was applied for 5 minutes.

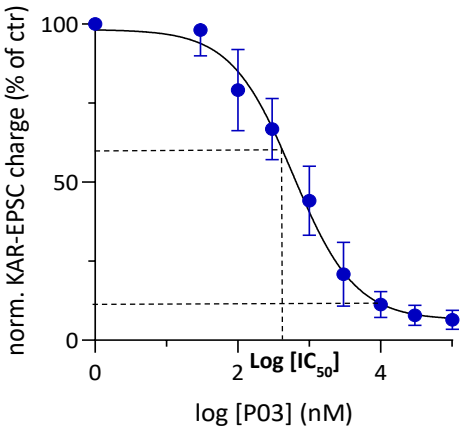

Figure 13 | Dose-response curve for P03 reducing KAR-EPSC synaptic charge; t_0 = 0 nM P03 → t_1=30 nM P03 → t_2 = 100 nM P03 → t_3 = 300 nM P03 → t_4 =1 µM P03 → t_5 P03 = 3 µM → t_6 = 10 µM → t_7 = 30 µM → t_8 = 100 µM; concentrations of P03 (nM) were transformed into a logarithmic scale; n=4-7 cells for each concentration.

In this dose-response curve, each data point represents 4 to 7 cells. It was observed that the effect of P03 reached its bottom *plateau* in reducing the synaptic charge of KAR-EPSCs around a concentration of 10 µM. The IC_{50} value for P03 automatically calculated using Prism – GraphPad was 590 nM.

4.2. P03 is not fully selective for GluK2/GluK5 KAR

In order to test the selectivity of P03 for GluK2/GluK5 KARs at mf-CA3 synapses, Protocol 3 was applied (see Materials and Methods) using a P03 concentration of 10 µM. With this protocol, it was possible to indirectly test whether P03 also affects presynaptic KARs (GluK2/GluK3) and/or postsynaptic AMPARs at mf-CA3 synapses. Several parameters were analysed in a new experimental group of recorded CA3 PCs (n=11), namely: 1) extent of frequency facilitation at mf-CA3 synapses before and after P03 application (considering for this calculation the AMPA+KAR EPSC peak amplitude at 3 Hz (average of 50 traces)) and the AMPA+KAR EPSC peak amplitude of the first pulse of paired-pulse (PP_1) (average of 30 traces)

(Fig. 14A); 2) the ratio of paired-pulse (PP40) stimulation, before and after P03 application (Fig. 14B) and 3) AMPA+KAR EPSC peak amplitude of PP_1, before and after P03 application (Fig. 14C).

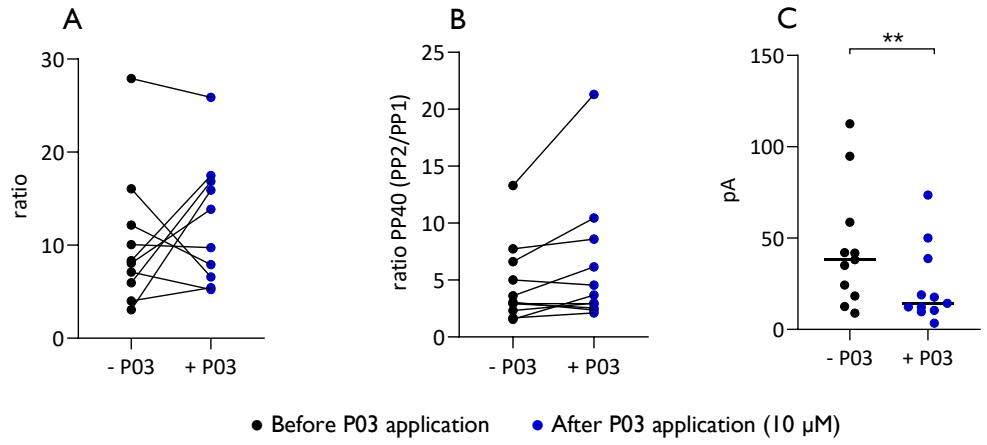

Figure 14 | P03 is not fully selective for GluK2/GluK5 KAR-EPSCs. **A** Frequency facilitation (FF) ratio before and after P03 application (paired t test, n=11, P>0.05 (ns)); **B** Ratio PP40 (PP2/PP1) before and after P03 application (paired t test, n=11, P>0.05 (ns)); **C** AMPA+KAR EPSCs peak amplitude of PP1, before and after P03 application (means values are represented as a black bar (before: 44 ± 10 pA; after: 24 ± 6 pA); Wilcoxon test, n=11, P<0.01 (**)).

These analyses demonstrate that P03 does not impact significantly FF or PP40 ratio at mf-CA3 synapses, and its effects are highly variable (Fig. 14A, B). On the other hand, it can be observed that P03 significantly reduces the AMPA+KAR-EPSCs peak amplitude of the first pulse in PP40 (PP_1) (from 44 ± 10 pA to 24 ± 6 pA). The decrease in AMPA+KAR EPSC by P03 indicates that the compound may also act on postsynaptic AMPA receptors, but not on presynaptic KARs since presynaptic plasticity is unchanged. The effect on AMPARs need to be further tested at synapses which do not express KARs.

IV. DISCUSSION

Along the Results section, several electrophysiology protocols were performed to evaluate the effect of new compounds targeting at KARs on both AMPA+KAR EPSCs and KAR-EPSCs. We analysed peak amplitudes, synaptic charge and decay times; it is important to distinguish the different type of information that can be extrapolated from each one of these parameters (although complementary). Thus, while EPSC peak amplitude analysis gave us the possibility to understand if the experimental compound had a direct effect on KAR-EPSCs peak amplitudes (Protocol 1), and/or on AMPA+KAR EPSCs peak amplitudes (Protocol 3) impacting fast excitatory neurotransmission, synaptic charge analysis allowed us to better understand the extension in the reduction of KAR-EPSCs in time. In this context, analyses of decay times are a good complementary analysis to justify differences between peak amplitude analysis and charge analysis, as well as to better characterize the receptors kinetics. A reduction in KAR-EPSC synaptic charge, as well as a reduction in its decay time, are very important features that these experimental compounds may display, considering the importance that GluK2/GluK5 KARs slow-mediated currents have in epileptic seizures. Blocking these slow currents (which contribute largely to the overall charge) might result in a very suitable therapeutic option in an epilepsy context, specifically temporal lobe epilepsy.

The first sets of analyses done both for the group of putative orthosteric antagonists of GluK2/GluK5 KARs (1.1.) and for putative allosteric modulators of GluK2/GluK5 KARs (2.1.) were important to guarantee that these mf-CA3 synapses were responding in a similar physiological way in every experimental group, having comparable synaptic parameters. No biologically significant differences were found between each CA3 PCs group regarding the extent of release at 0.1 Hz, frequency facilitation and overall receptors distribution (KARs and AMPARs).

As previously described, UBP310 (3 μM) was the first compound to be tested and it was used as a positive control, once this compound is known to be an antagonist of GluK2/GluK5 KARs. However, the reason this compound is limiting is mainly due to its lack of selectivity, since it acts also on GluK1 and GluK3 KARs. Thus, after testing UBP310, the main goal of this Master thesis was to find a molecule that could be as effective or that could overcome UBP310 effect on reducing KAR-EPSCs peak amplitudes (to 37% ± 3%) and, especially, synaptic charges (to 19 ± 2%) together with decay times (-71 ± 3%).

The results obtained in 1.3. regarding putative orthosteric antagonists, show that P03 (20 μM) is the most potent experimental compound inhibiting KAR-EPSCs. This could be observed not only by looking to the average remaining KAR-EPSCs peak amplitude (34 ± 3%) after compound application, but also by looking to the average remaining KAR-EPSCs synaptic charge

(14 ± 2%) and to the reduction in decay times (-71 ± 3%). This KAR-EPSCs inhibition was stronger than the results found in 1.2. for UBP310, however, we should take into consideration that the concentrations tested were different. Nevertheless, this set of results placed P03 as a lead compound among putative orthosteric antagonists. In the following Results topic (2.), a different group of compounds was tested, this time, putative allosteric modulators of GluK2/GluK5 KARs. Even though these compounds were firstly designed to be positive allosteric modulators of GluK2/GluK5 KARs as firstly described, they interestingly turned out to reduce the overall KAR-EPSCs at mf-CA3 synapses, having a more noticeable effect on the decrease of KAR-EPSCs peak amplitudes (ATM 2_21: 75 ± 4%; ATM 2_32: 83 ± 6 %) than on the reduction of the overall synaptic charge (ATM 2_21: 82 ± 6%; ATM 2_32: 103 ± 7%). Regarding the decay times measured, both compounds increased them (ATM 2_21: 27 ± 11%; ATM 2_32: 66 ± 26%).

Regarding the comparative analysis between each group of compounds described in section 3., it was possible to distinguish two main groups. A group of compounds that moderately reduced KAR-EPSCs synaptic charges and, at the same time, slowed down these currents (increased their decay times) (ATM 2_21, ATM 2_32 and LCKE10) and another group of compounds that strongly reduced KAR-EPSCs synaptic charges and, at the same time, decreased their decay times (UBP310, LC29 and P03). Here, it is relevant to highlight that LCKE10 (putative orthosteric antagonist) had a similar effect to putative allosteric modulators. These distinct effects might be linked with the KARs subtype which is being preferentially inhibited, however, further analysis with Protocol 3 and/or with recombinant KARs expressed in a heterologous expression system (e.g. HEK cells) would be needed to be performed to test this hypothesis for every compound.

Taking into account that the results obtained for putative orthosteric antagonists were more pronounced than for putative allosteric modulators, the following experiments focused only on putative orthosteric antagonists, specifically P03, the lead compound. Comparing the molecular structure of UBP310 and P03, the main differences lie in the right moiety of the molecule, where instead of a thiophene ring (C_4H_4S) with a carboxylic function, P03 has a benzene ring (C_6H_6) with a carboxylic function (see Materials and Methods).

In the following set of experiments (section 4.), it was established a dose-response curve for P03 in order to find the concentration in which this compound had its maximum effect on reducing KAR-EPSCs synaptic charge, as well as its IC_{50} value. Both these values were determined and were 10 μM and 590 nM, respectively. In order to test the selectivity of P03 for GluK2/GluK5 KARs, Protocol 3 was applied in section 4.2, using P03 at 10 μM. According to these results, P03 did not affect significantly FF and PP ratio at mf-CA3 synapses, suggesting that likely this compound is not acting on the presynaptic GluK2/GluK3 KARs, not affecting these two forms of hippocampal mossy fiber short-term plasticity. On the other hand, this compound

decreased the extent of synaptic release, slightly reducing the AMPA+KAR-EPSCs peak amplitude of the first pulse in PP40 (PP_1), being this last effect statistically significant. These last results are consistent with a possible effect of this antagonist on AMPA receptors, which are known to be present at postsynaptic level at mf-CA3 synapses, mediating fast excitatory neurotransmission. Further analysis to confirm these results will be need, such as testing the compound at synapses which do not express KARs.

Finally, there are some variables which should be taken into consideration while interpreting previous results. First, the nature of the electrophysiology protocols used (for instance, applying a protocol with a 3 Hz stimulation), and second, the possible/probable competitive nature of the experimental compound with glutamate might be an important to feature to considerate, once the glutamate concentration in the synaptic cleft is higher upon several stimulations. Nevertheless, the results obtained for UBP310 (which is known to be a competitive antagonist of GluK2/GluK5 KAR) were quite similar to previous works (Pinheiro *et al*., 2013), considering synaptic charge data analysis. Additionally, the incomplete blockade of AMPA receptors by LY303070 (25 μm) might also be a possibility to considerate, meaning that the measured currents can be partially AMPAR-EPSCs and not KAR-EPSCs. Finally, it should also be taken into account the variability that exists in a physiologic context, including the size of each mf-CA3 synapse, the number of kainate receptors in each one, and the subtypes of kainate receptors present in pre- and postsynaptic regions.

V. CONCLUSIONS AND FUTURE PERSPECTIVES

Temporal lobe epilepsy is the most common focal (localization-related) epilepsy known nowadays, affecting mainly the hippocampus. More than 30% of these epileptic patients become refractory to current AEDs on the market. Surgical procedures, stimulation of vagus nerve or responsive neurostimulation are the remaining alternative clinical approaches to alleviate these patients' symptomatology. Recently, heteromeric KARs containing GluK2/GluK5 subunits are emerging as new potential therapeutic targets in temporal lobe epilepsy. A major histopathological feature of TLE patients' hippocampal tissue is the aberrant mossy fiber sprouting and these rMFs operate mostly via GluK2/GluK5 KARs. Mainly due to their slow kinetics and small amplitude currents, GluK2/GluK5 KARs can change DGCs firing regime, switching their sparse firing mode to a sustained firing one, increasing the excitability of DGCs. Thus, it has been clearly demonstrated that these ectopic KARs contribute either to the acute epileptiform activity and to chronic and recurrent epileptic seizures.

Nowadays, only a few useful orthosteric antagonists or allosteric modulators that selectively inhibit KARs and spare AMPARs are available, since KARs and AMPARs exhibit overlapping sensitivities to most of these compounds (Contractor *et al*., 2011; Jane *et al.,* 2009). Hence, the absence of such selective pharmacological tools hampers not only the development of an alternative therapeutic option for some patients, as well as it creates serious limitations to characterize the physiological functions of neuronal KARs. The existence of splice variants and editing sites on KARs subunits further increases the likelihood of pharmacological heterogeneity (Jane *et al.,* 2009). These studies on pharmacology have been aided by the availability of KAR knockouts. Each approach has its relative advantages and disadvantages but in combination they are extremely powerful. Thus, the use of both pharmacology and knockout mice to understand KAR function has been the subject of several recent reviews (Larsen *et al*., 2017).

In this Master thesis, two main classes of pharmacological compounds targeting GluK2/GluK5 KARs were explored: putative orthosteric antagonists and putative allosteric modulators. Among all the compounds and experiments performed, P03, a putative orthosteric antagonist of GluK2/GluK5 KARs, was the pharmacological compound presenting more interesting and encouraging results. Despite the fact of these experiments strongly suggest that this compound is not fully selective for GluK2/GluK5, acting also on AMPARs, this hypothesis should be further explored. There are several experiments that could be performed, namely:

a. Testing the effect of P03 (10 μM) on A/C synapses at CA3 pyramidal cells; knowing that these synapses do not contain KARs both in pre- and postsynaptic sites (Rebola *et al*., 2017), this would be a possible set of experiments to test P03 effect on AMPARs;

b. Performing the same experiments as described in Protocol 3 but with KO mice for GluK2 subunit;
c. Expressing heteromeric GluK2/GluK5 KARs, GluK2/GluK3 or homomeric GluK2/GluK2 in a heterologous recombinant system (e.g. HEK cells) and do patch-clamp on these cells (e.g. whole cell patch-clamp), comparing their electrophysiological response to glutamate after a prior P03 bath application (10 μM);
d. Testing of P03 in epileptic slices or TLE animal models.

These and other experiments might be performed in order to better characterize P03 and its selectivity both to GluK2/GluK5, GluK2/GluK3 and also AMPA receptors. In fact, a compound that could act both on GluK2/GluK5 KARs and AMPARs could still be an interesting compound to test in a temporal lobe epilepsy context (epileptic slices or animal models). For instance, perampanel is a commercially available drug for epilepsy and its main mechanism of action is thought to be through non-competitive AMPA-glutamate receptor antagonism.

There is still a considerable amount of questions unanswered: 1) Which are the mechanisms involved in the recruitment of aberrant KARs at rMF-DGC synapses?; 2) Which are the consequences of GluK2/GluK5 receptor inhibition on neuronal processing in CA3 in epileptic conditions? And in other brain regions containing this KAR subtype? Which are the main clinical adverse events on healthy humans and epileptic patients?; 3) What roles do KARs play in network activity and higher cognitive brain functions?; 4) Do KARs play a significant role in neuropsychiatric and neurological disorders?

These and other questions remain to be answered. Finding new antagonists or allosteric modulators selective to each KAR subunit will allow not only the development of new pharmacological tools for better therapeutic regimens in temporal lobe epilepsy and other neuropathologies, but also will allow the detailed study of physiological role of each KAR subunit and each KAR subtype.

SUPPLEMENTARY DATA

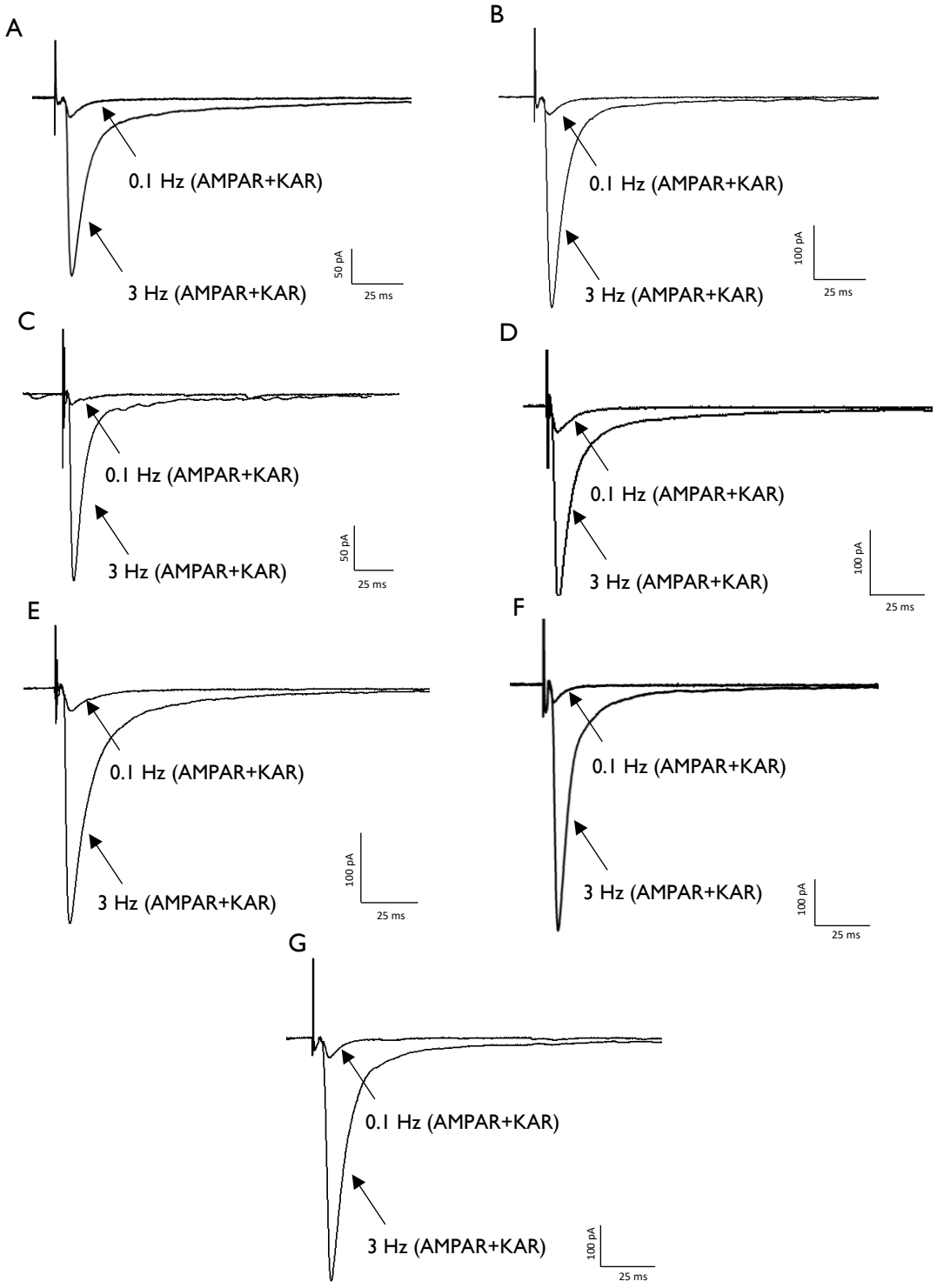

Supplementary Figure 1 | Frequency facilitation at mf-CA3 synapses. Representative traces of pharmacologically isolated AMPA+KAR EPSCs at 0.1 Hz and 3 Hz (average of 30 and 50 traces, respectively) at mf-CA3 synapses, prior to UBP310 (Fig 1A), LCKE10 (Fig. 1B), LC29 (Fig. 1C), P03 (Fig. 1D), BPAM344 (Fig. 1E), ATM 2_21 (Fig. 1F) and ATM 2_32 (Fig. 1G) application. For every compound, it can be observed a large frequency facilitation at mf-CA3 synapse.

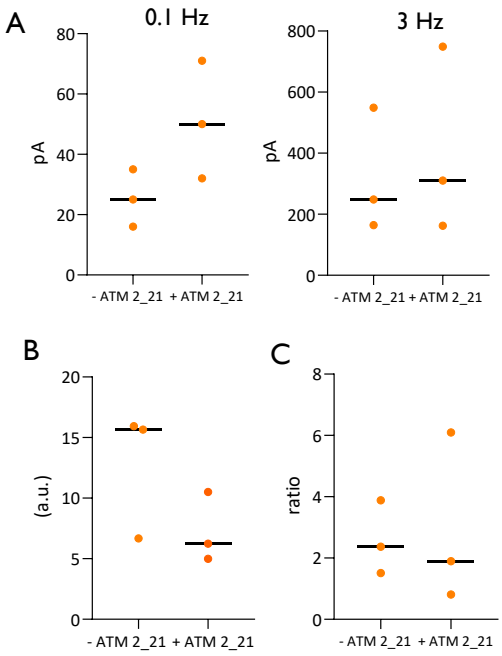

Supplementary Figure 2 | ATM 2_21 increases AMPA+KAR EPSCs baseline (0.1 Hz and 3 Hz stimulations) (Fig. 2A), decreases frequency facilitation (Fig. 2B) and decreases paired-pulse ratio (Fig. 2C) (n=3) at mf-CA3 synapses.

REFERENCES

Artinian, J., Peret, A., Marti, G., Epsztein, J., & Crépel, V. (2011). Synaptic kainate receptors in interplay with INaP shift the sparse firing of dentate granule cells to a sustained rhythmic mode in temporal lobe epilepsy. *Journal of Neuroscience*, *31*(30), 10811–10818. https://doi.org/10.1523/JNEUROSCI.0388-11.2011

Banke, T. G., & Gegelashvili, G. (2008). Tonic activation of group I mGluRs modulates inhibitory synaptic strength by regulating KCC2 activity. *Journal of Physiology*, *586*(20), 4925–4934. https://doi.org/10.1113/jphysiol.2008.157024

Barberis, A., Sachidhanandam, S., & Mulle, C. (2008). GluR6/KA2 kainate receptors mediate slow-deactivating currents. *Journal of Neuroscience*, *28*(25), 6402–6406. https://doi.org/10.1523/JNEUROSCI.1204-08.2008

Bettler, B., Boulter, J., Hermans-Borgmeyer, I., O'Shea-Greenfield, A., Deneris, E. S., Moll, C., Borgmeyer, U., Hollmann, M., & Heinemann, S. (1990). Cloning of a novel glutamate receptor subunit, GluR5: expression in the nervous system during development. *Neuron*, *5*(5), 583–595. https://doi.org/10.1016/0896-6273(90)90213-y

Bischofberger, J., & Schinder, A. F. (2008). Maturation and Functional Integration of New Granule Cells into the Adult Hippocampus. *Cold Spring Harbor Monograph Archive*, *52*, 299–319. https://doi.org/10.1101/087969784.52.299

Blair, R. D. G. (2012). Temporal Lobe Epilepsy Semiology. *Epilepsy Research and Treatment*, *2012*, 1–10. https://doi.org/10.1155/2012/751510

Bleakman, D., & Lodge, D. (1998). Neuropharmacology of AMPA and kainate receptors. *Neuropharmacology*, *37*(10–11), 1187–1204. https://doi.org/10.1016/S0028-3908(98)00139-7

Bowie, D. (2002). External anions and cations distinguish between AMPA and kainate receptor gating mechanisms. *Journal of Physiology*, *539*(3), 725–733. https://doi.org/10.1113/jphysiol.2001.013407

Bowie, D. (2010). Ion-dependent gating of kainate receptors. *Journal of Physiology*, *588*(1), 67–81. https://doi.org/10.1113/jphysiol.2009.178863

Bräuner-Osborne, H., Egebjerg, J., Nielsen, E., Madsen, U., & Krogsgaard-Larsen, P. (2000). Ligands for glutamate receptors: Design and therapeutic prospects. *Journal of Medicinal Chemistry*, *43*(14), 2609–2645. https://doi.org/10.1021/jm000007r

Bureau, I., Bischoff, S., Heinemann, S. F., & Mulle, C. (1999). Kainate receptor-mediated responses in the CA1 field of wild-type and GluR6-deficient mice. *Journal of Neuroscience*, *19*(2), 653–663. https://doi.org/10.1523/jneurosci.19-02-00653.1999

Carta, M., Fièvre, S., Gorlewicz, A., & Mulle, C. (2014). Kainate receptors in the hippocampus. *European Journal of Neuroscience*, *39*(11), 1835–1844. https://doi.org/10.1111/ejn.12590

Chang, R. S. kwan, Leung, C. Y. W., Ho, C. C. A., & Yung, A. (2017). Classifications of seizures and epilepsies, where are we? – A brief historical review and update. *Journal of the Formosan Medical Association*, *116*(10), 736–741. https://doi.org/10.1016/j.jfma.2017.06.001

Chorin, E., Vinograd, O., Fleidervish, I., Gilad, D., Herrmann, S., Sekler, I., Aizenman, E., & Hershfinkel, M. (2011). Upregulation of KCC2 activity by zinc-mediated neurotransmission via the mZnR/GPR39 receptor. *The Journal of neuroscience : the official journal of the Society for Neuroscience*, *31*(36), 12916–12926. https://doi.org/10.1523/JNEUROSCI.2205-11.2011

Contractor, A., Swanson, G. T., Sailer, A., O'Gorman, S., & Heinemann, S. F. (2000). Identification of the kainate receptor subunits underlying modulation of excitatory synaptic transmission in the CA3 region of the hippocampus. *Journal of Neuroscience*, *20*(22), 8269–8278. https://doi.org/10.1523/jneurosci.20-22-08269.2000

Contractor, Anis, Mulle, C., & Swanson, G. T. (2011). Kainate receptors coming of age: Milestones of two decades of research. *Trends in Neurosciences*, *34*(3), 154–163. https://doi.org/10.1016/j.tins.2010.12.002

Contractor, Anis, Sailer, A. W., Darstein, M., Maron, C., Xu, J., Swanson, G. T., & Heinemann, S. F. (2003). Loss of Kainate Receptor-Mediated Heterosynaptic Facilitation of Mossy-Fiber Synapses in KA2 −/− Mice . *The Journal of Neuroscience*, *23*(2), 422–429. https://doi.org/10.1523/jneurosci.23-02-00422.2003

Contractor, Anis, Swanson, G., & Heinemann, S. F. (2001). Kainate receptors are involved in short- and long-term plasticity at mossy fiber synapses in the hippocampus. *Neuron*, *29*(1), 209–216. https://doi.org/10.1016/S0896-6273(01)00191-X

Copits, B. A., & Swanson, G. T. (2012). Dancing partners at the synapse: Auxiliary subunits that shape kainate receptor function. *Nature Reviews Neuroscience*, *13*(10), 675–686. https://doi.org/10.1038/nrn3335

Coussen, F., Normand, E., Marchal, C., Costet, P., Choquet, D., Lambert, M., Mège, R. M., & Mulle, C. (2002). Recruitment of the kainate receptor subunit glutamate receptor 6 by cadherin/catenin complexes. *The Journal of neuroscience : the official journal of the Society for Neuroscience*, *22*(15), 6426–6436. https://doi.org/10.1523/JNEUROSCI.22-15-06426.2002

Crépel, V., & Mulle, C. (2015). Physiopathology of kainate receptors in epilepsy. *Current Opinion in Pharmacology*, *20*, 83–88. https://doi.org/10.1016/j.coph.2014.11.012

Dawe, G. B., Musgaard, M., Andrews, E. D., Daniels, B. A., Aurousseau, M. R. P., Biggin, P. C., & Bowie, D. (2013). Defining the structural relationship between kainate-receptor deactivation and desensitization. *Nature Structural and Molecular Biology*, *20*(9), 1054–1061. https://doi.org/10.1038/nsmb.2654

Devinsky, O., Spruill, T., Thurman, D., & Friedman, D. (2016). Recognizing and Preventing Epilepsy-Related Mortality: A Call for Action. *Neurology*, *86*(8), 779–786. Retrieved from http://www.neurology.org/content/86/8/779.full.pdf

Dolman, N. P., More, J. C., Alt, A., Knauss, J. L., Pentikäinen, O. T., Glasser, C. R., Bleakman, D., Mayer, M. L., Collingridge, G. L., & Jane, D. E. (2007). Synthesis and pharmacological characterization of N3-substituted willardiine derivatives: role of the substituent at the 5-position of the uracil ring in the development of highly potent and selective GLUK5 kainate receptor antagonists. *Journal of medicinal chemistry*, *50*(7), 1558–1570. https://doi.org/10.1021/jm061041u

Epsztein, J. (2005). Recurrent Mossy Fibers Establish Aberrant Kainate Receptor-Operated Synapses on Granule Cells from Epileptic Rats. *Journal of Neuroscience*, *25*(36), 8229–8239. https://doi.org/10.1523/jneurosci.1469-05.2005

Fièvre, S., Carta, M., Chamma, I., Labrousse, V., Thoumine, O., & Mulle, C. (2016). Molecular determinants for the strictly compartmentalized expression of kainate receptors in CA3 pyramidal cells. *Nature Communications*, *7*. https://doi.org/10.1038/ncomms12738

Fisher, R. S., Acevedo, C., Arzimanoglou, A., Bogacz, A., Cross, J. H., Elger, C. E., Engel, J., Jr, Forsgren, L., French, J. A., Glynn, M., Hesdorffer, D. C., Lee, B. I., Mathern, G. W., Moshé, S. L., Perucca, E., Scheffer, I. E., Tomson, T., Watanabe, M., & Wiebe, S. (2014). ILAE official report: a practical clinical definition of epilepsy. *Epilepsia*, *55*(4), 475–482. https://doi.org/10.1111/epi.12550

Fukushima, T., Shingai, R., Ogurusu, T., & Ichinose, M. (2003). Inhibition of willardiine-induced currents through rat GluR6/KA-2 kainate receptor channels by Zinc and other divalent cations. *Neuroscience Letters*, *349*(2), 107–110. https://doi.org/10.1016/S0304-3940(03)00805-X

Gallyas, F., Ball, S. M., & Molnar, E. (2003). Assembly and cell surface expression of KA-2 subunit-containing kainate receptors. *Journal of Neurochemistry*, *86*(6), 1414–1427. https://doi.org/10.1046/j.1471-4159.2003.01945.x

Gano, L. B., Liang, L. P., Ryan, K., Michel, C. R., Gomez, J., Vassilopoulos, A., Reisdorph, N., Fritz, K. S., & Patel, M. (2018). Altered mitochondrial acetylation profiles in a kainic acid model of temporal lobe epilepsy. *Free radical biology & medicine*, *123*, 116–124. https://doi.org/10.1016/j.freeradbiomed.2018.05.063

Garand, D., Mahadevan, V., & Woodin, M. A. (2019). Ionotropic and metabotropic kainate receptor signalling regulates Cl^- homeostasis and GABAergic inhibition. *The Journal of physiology*, *597*(6), 1677–1690. https://doi.org/10.1113/JP276901

González-González, I. M., Konopacki, F. A., Rocca, D. L., Doherty, A. J., Jaafari, N., Wilkinson, K. A., & Henley, J. M. (2012). Kainate receptor trafficking. *Wiley Interdisciplinary Reviews: Membrane Transport and Signaling*, *1*(1), 31–44. https://doi.org/10.1002/wmts.23

Hadera, M. G., Eloqayli, H., Jaradat, S., Nehlig, A., & Sonnewald, U. (2015). Astrocyte-neuronal interactions in epileptogenesis. *Journal of Neuroscience Research*, *93*(7), 1157–1164. https://doi.org/10.1002/jnr.23584

Hauser, R. M., Henshall, D. C., & Lubin, F. D. (2018). The Epigenetics of Epilepsy and Its Progression. *Neuroscientist*, *24*(2), 186–200. https://doi.org/10.1177/1073858417705840

Helbig, I., & Lowenstein, D. H. (2013). Genetics of the epilepsies: Where are we and where are we going? *Current Opinion in Neurology*, *26*(2), 179–185. https://doi.org/10.1097/WCO.0b013e32835ee6ff

Hollmann, M., Maron, C., & Heinemann, S. (1994). N-glycosylation site tagging suggests a three transmembrane domain topology for the glutamate receptor GluRI. *Neuron*, *13*(6), 1331–1343. https://doi.org/10.1016/0896-6273(94)90419-7

Huettner, J. E., Stack, E., & Wilding, T. J. (1998). Antagonism of neuronal kainate receptors by lanthanum and gadolinium. *Neuropharmacology*, *37*(10–11), 1239–1247. https://doi.org/10.1016/S0028-3908(98)00082-3

Jane, D. E., Lodge, D., & Collingridge, G. L. (2009). Kainate receptors: Pharmacology, function and therapeutic potential. *Neuropharmacology*, *56*(1), 90–113. https://doi.org/10.1016/j.neuropharm.2008.08.023

Kahle, K. T., Merner, N. D., Friedel, P., Silayeva, L., Liang, B., Khanna, A., Shang, Y., Lachance-Touchette, P., Bourassa, C., Levert, A., Dion, P. A., Walcott, B., Spiegelman, D., Dionne-Laporte, A., Hodgkinson, A., Awadalla, P., Nikbakht, H., Majewski, J., Cossette, P., Deeb, T. Z., … Rouleau, G. A. (2014). Genetically encoded impairment of neuronal KCC2 cotransporter function in human idiopathic generalized epilepsy. *EMBO reports*, *15*(7), 766–774. https://doi.org/10.15252/embr.201438840

Kerchner, G. A., Wilding, T. J., Huettner, J. E., & Zhuo, M. (2002). Kainate receptor subunits underlying presynaptic regulation of transmitter release in the dorsal horn. *Journal of Neuroscience*, *22*(18), 8010–8017. https://doi.org/10.1523/jneurosci.22-18-08010.2002

Kew, J. N. C., & Kemp, J. A. (2005). Ionotropic and metabotropic glutamate receptor structure and pharmacology. *Psychopharmacology*, *179*(1), 4–29. https://doi.org/10.1007/s00213-005-2200-z

Kohda, K., Kakegawa, W., Matsuda, S., Yamamoto, T., Hirano, H., & Yuzaki, M. (2013). The δ2 glutamate receptor gates long-term depression by coordinating interactions between two AMPA receptor phosphorylation sites. *Proceedings of the National Academy of Sciences of the United States of America*, 110(10), E948–E957. https://doi.org/10.1073/pnas.1218380110

Larsen, A. M., & Bunch, L. (2011). Medicinal chemistry of competitive kainate receptor antagonists. *ACS Chemical Neuroscience*, *2*(2), 60–74. https://doi.org/10.1021/cn1001039

Larsen, A. P., Fièvre, S., Frydenvang, K., Francotte, P., Pirotte, B., Kastrup, J. S., & Mulle, C. (2017). Identification and structure-function study of positive allosteric modulators of kainate receptors. *Molecular Pharmacology*, *91*(6), 576–585. https://doi.org/10.1124/mol.116.107599

Lerma, J., & Marques, J. M. (2013). Kainate receptors in health and disease. *Neuron*, *80*(2), 292–311. https://doi.org/10.1016/j.neuron.2013.09.045

Lévesque, M., & Avoli, M. (2013). The kainic acid model of temporal lobe epilepsy. *Neuroscience and Biobehavioral Reviews*, *37*(10), 2887–2899. https://doi.org/10.1016/j.neubiorev.2013.10.011

Lévesque, M., Avoli, M., & Bernard, C. (2016, February 15). Animal models of temporal lobe epilepsy following systemic chemoconvulsant administration. *Journal of Neuroscience Methods*, Vol. 260, pp. 45–52. https://doi.org/10.1016/j.jneumeth.2015.03.009

Mahadevan, V., Pressey, J. C., Acton, B. A., Uvarov, P., Huang, M. Y., Chevrier, J., Puchalski, A., Li, C. M., Ivakine, E. A., Airaksinen, M. S., Delpire, E., McInnes, R. R., & Woodin, M. A. (2014). Kainate receptors coexist in a functional complex with KCC2 and regulate chloride homeostasis in hippocampal neurons. *Cell reports*, *7*(6), 1762–1770. https://doi.org/10.1016/j.celrep.2014.05.022

Mahadevan, V., & Woodin, M. A. (2016). Regulation of neuronal chloride homeostasis by neuromodulators. *Journal of Physiology*, *594*(10), 2593–2605. https://doi.org/10.1113/JP271593

Matsuda, K., Budisantoso, T., Mitakidis, N., Sugaya, Y., Miura, E., Kakegawa, W., Yamasaki, M., Konno, K., Uchigashima, M., Abe, M., Watanabe, I., Kano, M., Watanabe, M., Sakimura, K., Aricescu, A. R., & Yuzaki, M. (2016). Transsynaptic Modulation of Kainate Receptor Functions by C1q-like Proteins. *Neuron*, *90*(4), 752–767. https://doi.org/10.1016/j.neuron.2016.04.001

Mayer, M. L., Ghosal, A., Dolman, N. P., & Jane, D. E. (2006). Crystal structures of the kainate receptor GluR5 ligand binding core dimer with novel GluR5-selective antagonists. *Journal of Neuroscience*, *26*(11), 2852–2861. https://doi.org/10.1523/JNEUROSCI.0123-06.2005

Melyan, Z., Wheal, H. V., & Lancaster, B. (2002). Metabotropic-mediated kainate receptor regulation of IsAHP and excitability in pyramidal cells. *Neuron*, *34*(1), 107–114. https://doi.org/10.1016/S0896-6273(02)00624-4

Mulle, C., Sailer, A., Pérez-Otaño, I., Dickinson-Anson, H., Castillo, P. E., Bureau, I., Maron, C., Gage, F. H., Mann, J. R., Bettler, B., & Heinemann, S. F. (1998). Altered synaptic physiology and reduced susceptibility to kainate-induced seizures in GluR6-deficient mice. *Nature*, *392*(6676), 601–605. https://doi.org/10.1038/33408

Møllerud, S., Frydenvang, K., Pickering, D. S., & Kastrup, J. S. (2017, January 1). Lessons from crystal structures of kainate receptors. *Neuropharmacology*, Vol. 112, pp. 16–28. https://doi.org/10.1016/j.neuropharm.2016.05.014

Neligan, A., Hauser, W. A., & Sander, J. W. (2012). The epidemiology of the epilepsies. In *Handbook of Clinical Neurology* (1st ed., Vol. 107). https://doi.org/10.1016/B978-0-444-52898-8.00006-9

Nicolas W. Cortes-Penfield, Barbara W. Trautner, R. J. (2017). S. Zhu, E. Gouaux, Structure and symmetry inform gating principles of ionotropic glutamate receptors, Neuropharmacology. 112 (2017) 11–15. doi:10.1016/J.NEUROPHARM.2016.08.034. *Physiology & Behavior*, *176*(5), 139–148. https://doi.org/10.1016/j.physbeh.2017.03.040

Nirwan, N., Vyas, P., & Vohora, D. (2018). Animal models of status epilepticus and temporal lobe epilepsy: A narrative review. *Reviews in the Neurosciences*, *29*(7), 757–770. https://doi.org/10.1515/revneuro-2017-0086

Paramo, T., Brown, P. M. G. E., Musgaard, M., Bowie, D., & Biggin, P. C. (2017). Functional Validation of Heteromeric Kainate Receptor Models. *Biophysical Journal*, *113*(10), 2173–2177. https://doi.org/10.1016/j.bpj.2017.08.047

Partin, K. M., Patneau, D. K., Winters, C. A., Mayer, M. L., & Buonanno, A. (1993). Selective modulation of desensitization at AMPA versus kainate receptors by cyclothiazide and concanavalin A. *Neuron*, *11*(6), 1069–1082. https://doi.org/10.1016/0896-6273(93)90220-L

Paternain, A. V., Cohen, A., Stern-Bach, Y., & Lerma, J. (2003). A role for extracellular Na+ in the channel gating of native and recombinant kainate receptors. *Journal of Neuroscience*, *23*(25), 8641–8648. https://doi.org/10.1523/jneurosci.23-25-08641.2003

Peret, A., Christie, L. A., Ouedraogo, D. W., Gorlewicz, A., Epsztein, J. Ô., Mulle, C., & Crépel, V. (2014). Contribution of Aberrant GluK2-Containing Kainate Receptors to Chronic Seizures in Temporal Lobe Epilepsy. *Cell Reports*, *8*(2), 347–354. https://doi.org/10.1016/j.celrep.2014.06.032

Perrais, D., Coussen, F., & Mulle, C. (2009). Atypical functional properties of GluK3-containing kainate receptors. *Journal of Neuroscience*, *29*(49), 15499–15510. https://doi.org/10.1523/JNEUROSCI.2724-09.2009

Perrais, D., Pinheiro, P. S., Jane, D. E., & Mulle, C. (2009). Antagonism of recombinant and native GluK3-containing kainate receptors. *Neuropharmacology*, *56*(1), 131–140. https://doi.org/10.1016/j.neuropharm.2008.08.002

Petrovic, M. M., Viana Da Silva, S., Clement, J. P., Vyklicky, L., Mulle, C., González-González, I. M., & Henley, J. M. (2017). Metabotropic action of postsynaptic kainate receptors triggers hippocampal long-term potentiation. *Nature Neuroscience*, *20*(4), 529–539. https://doi.org/10.1038/nn.4505

Pinheiro, P. S., Lanore, F., Veran, J., Artinian, J., Blanchet, C., Crépel, V., Perrais, D., & Mulle, C. (2013). Selective block of postsynaptic kainate receptors reveals their function at hippocampal mossy fiber synapses. *Cerebral cortex (New York, N.Y. : 1991)*, *23*(2), 323–331. https://doi.org/10.1093/cercor/bhs022

Pinheiro, P., & Mulle, C. (2006). Kainate receptors. *Cell and tissue research*, *326*(2), 457–482. https://doi.org/10.1007/s00441-006-0265-6

Pinheiro, P. S., Perrais, D., Coussen, F., Barhanin, J., Bettler, B., Mann, J. R., … Mulle, C. (2007). GluR7 is an essential subunit of presynaptic kainate autoreceptors at hippocampal mossy fiber synapses. *Proceedings of the National Academy of Sciences of the United States of America*, *104*(29), 12181–12186. https://doi.org/10.1073/pnas.0608891104

Pressey, J. C., Mahadevan, V., Khademullah, C. S., Dargaei, Z., Chevrier, J., Ye, W., Huang, M., Chauhan, A. K., Meas, S. J., Uvarov, P., Airaksinen, M. S., & Woodin, M. A. (2017). A kainate receptor subunit promotes the recycling of the neuron-specific K^+-Cl^- co-transporter KCC2 in hippocampal neurons. *The Journal of biological chemistry*, *292*(15), 6190–6201. https://doi.org/10.1074/jbc.M116.767236

Rebola, N., Carta, M., & Mulle, C. (2017). Operation and plasticity of hippocampal CA3 circuits: Implications for memory encoding. *Nature Reviews Neuroscience*, *18*(4), 209–221. https://doi.org/10.1038/nrn.2017.10

Reid, C. A., Berkovic, S. F., & Petrou, S. (2009). Mechanisms of human inherited epilepsies. *Progress in Neurobiology*, *87*(1), 41–57. https://doi.org/10.1016/j.pneurobio.2008.09.016

Reiner, A., Arant, R. J., & Isacoff, E. Y. (2012). Assembly stoichiometry of the GluK2/GluK5 kainate receptor complex. *Cell reports*, *1*(3), 234–240. https://doi.org/10.1016/j.celrep.2012.01.003

Ren, Z., Riley, N. J., Garcia, E. P., Sanders, J. M., Swanson, G. T., & Marshall, J. (2003). Multiple trafficking signals regulate kainate receptor KA2 subunit surface expression. *Journal of Neuroscience*, *23*(16), 6608–6616. https://doi.org/10.1523/jneurosci.23-16-06608.2003

Ricos, M. G., Hodgson, B. L., Pippucci, T., Saidin, A., Ong, Y. S., Heron, S. E., … Dibbens, L. M. (2016). Mutations in the mammalian target of rapamycin pathway regulators NPRL2 and NPRL3 cause focal epilepsy. *Annals of Neurology*, *79*(1), 120–131. https://doi.org/10.1002/ana.24547

Rodríguez-Moreno, A., & Lerma, J. (1998). Kainate receptor modulation of GABA release involves a metabotropic function. *Neuron*, *20*(6), 1211–1218. https://doi.org/10.1016/S0896-6273(00)80501-2

Rogawski, M. A., & Löscher, W. (2004). The neurobiology of antiepileptic drugs. *Nature Reviews Neuroscience*, *5*(7), 553–564. https://doi.org/10.1038/nrn1430

Ruiz, A., Sachidhanandam, S., Utvik, J. K., Coussen, F., & Mulle, C. (2005). Distinct subunits in heteromeric kainate receptors mediate ionotropic and metabotropic function at hippocampal mossy fiber synapses. *Journal of Neuroscience*, *25*(50), 11710–11718. https://doi.org/10.1523/JNEUROSCI.4041-05.2005

Scheffer, I. E., Berkovic, S., Capovilla, G., Connolly, M. B., French, J., Guilhoto, L., … Zuberi, S. M. (2018). ILAE classification of the epilepsies: position paper of the ILAE Commission for Classification and Terminology. *Zeitschrift Fur Epileptologie*, *31*(4), 296–306. https://doi.org/10.1007/s10309-018-0218-6

Scheffer, I. E., Heron, S. E., Regan, B. M., Mandelstam, S., Crompton, D. E., Hodgson, B. L., … Dibbens, L. M. (2014). Mutations in mammalian target of rapamycin regulator DEPDC5 cause focal epilepsy with brain malformations. *Annals of Neurology*, *75*(5), 782–787. https://doi.org/10.1002/ana.24126

Sheardown, M. J., Nielsen, E. O., Hansen, A. J., Jacobsen, P., & Honoré, T. (1990). 2,3-Dihydroxy-6-nitro-7-sulfamoyl-benzo(F)quinoxaline: a neuroprotectant for cerebral ischemia. *Science (New York, N.Y.)*, *247*(4942), 571–574. https://doi.org/10.1126/science.2154034

Symonds, J. D., Zuberi, S. M., & Johnson, M. R. (2017). Advances in epilepsy gene discovery and implications for epilepsy diagnosis and treatment. *Current Opinion in Neurology*, *30*(2), 193–199. https://doi.org/10.1097/WCO.0000000000000433

Thijs, R. D., Surges, R., O'Brien, T. J., & Sander, J. W. (2019). Epilepsy in adults. *The Lancet*, *393*(10172), 689–701. https://doi.org/10.1016/S0140-6736(18)32596-0

Traynelis, S. F., Wollmuth, L. P., McBain, C. J., Menniti, F. S., Vance, K. M., Ogden, K. K., Hansen, K. B., Yuan, H., Myers, S. J., & Dingledine, R. (2010). Glutamate receptor ion channels: structure, regulation, and function. *Pharmacological reviews*, *62*(3), 405–496. https://doi.org/10.1124/pr.109.002451

Venceslas, D., & Corinne, R. (2017). A Mesiotemporal Lobe Epilepsy Mouse Model. *Neurochemical Research*, *42*(7), 1919–1925. https://doi.org/10.1007/s11064-017-2239-3

Veran, J., Kumar, J., Pinheiro, P. S., Athané, A., Mayer, M. L., Perrais, D., & Mulle, C. (2012). Zinc Potentiates GluK3 Glutamate Receptor Function by Stabilizing the Ligand Binding Domain Dimer Interface. *Neuron*, *76*(3), 565–578. https://doi.org/10.1016/j.neuron.2012.08.027

Vincent, P., & Mulle, C. (2009). Kainate receptors in epilepsy and excitotoxicity. *Neuroscience*, *158*(1), 309–323. https://doi.org/10.1016/j.neuroscience.2008.02.066

Watkins, J C, & Evans, R. H. (2003). Excitatory Amino Acid Transmitters. *Annual Review of Pharmacology and Toxicology*, *21*(1), 165–204. https://doi.org/10.1146/annurev.pa.21.040181.001121

Watkins, Jeffrey C., & Jane, D. E. (2006). The glutamate story. *British Journal of Pharmacology*, *147*(SUPPL. 1), 100–108. https://doi.org/10.1038/sj.bjp.0706444

Weckhuysen, S., Marsan, E., Lambrecq, V., Marchal, C., Morin-Brureau, M., An-Gourfinkel, I., Baulac, M., Fohlen, M., Kallay Zetchi, C., Seeck, M., de la Grange, P., Dermaut, B., Meurs, A., Thomas, P., Chassoux, F., Leguern, E., Picard, F., & Baulac, S. (2016). Involvement of GATOR complex genes in familial focal epilepsies and focal cortical dysplasia. *Epilepsia*, *57*(6), 994–1003. https://doi.org/10.1111/epi.13391

Wong, A. Y. C., Fay, A. M. L., & Bowie, D. (2006). External ions are coactivators of kainate receptors. *Journal of Neuroscience*, *26*(21), 5750–5755. https://doi.org/10.1523/JNEUROSCI.0301-06.2006